J. Math. Computer Sci., 29 (2023), 214–238

Online: ISSN 2008-949X

Journal of Mathematics and Computer Science

Journal Homepage: www.isr-publications.com/jmcs

Infection dynamics of rabbit and red fox with alternative prey

Jyoti Gupta[a,*], Joydip Dhar[b], Poonam Sinha[a]

[a]S.M.S. Govt. Model Science College, Jiwaji University, Gwalior-474002, M.P., India.

[b]ABV-Indian Institute of Information Technology and Management, Gwalior-474015, M.P., India.

Abstract

In many countries, the decline in red foxes due to Rabbit hemorrhagic disease (RHD) in primary prey European rabbits is a significant concern. We proposed a four-compartment spatiotemporal rabbits-alternative prey-red fox eco-epidemiological model with mange disease and hunting in red foxes. The essential theoretical properties, such as existence, boundedness, stability, and bifurcation analysis, are executed. We have also conducted Turing instability and Higher-order stability analysis for the spatiotemporal model. Hopf bifurcation is shown at a critical value of hunting rate $h = h_c$ using central manifold theory. Numerical simulation reveals that the present dynamic is chaotic for a mange disease transmission rate's threshold value $\beta = \beta_+$, the most significant factor in the present dynamics. We can control the red fox population by controlling the mange contact rate despite RHD disease in European rabbits. Also, the model does not have diffusion-driven instability due to alternative prey, and if the system is linearly stable, it remains stable for higher-order.

Keywords: Stability, bifurcation, mange, chaos.

2020 MSC: 34C23, 34D20, 92B05, 92D30.

©2023 All rights reserved.

1. Introduction

The red fox is one of the most widely distributed wild carnivores in Eurasia, North America, and Australia [3, 15]. The red foxes are opportunistic predators as the amount and type of food consumed by them are just dependent on the supply only [1]. Generally, they feed on rabbits, bunnies, small birds, wild fruits, and berries [1], but the rabbits act as primary prey for red foxes due to moderate size and accessibility.

Rabbit hemorrhagic disease (RHD) is a highly infectious and fatal disease of wild and domestic rabbits. It is a horizontally transmitted disease with no recovery [28, 29, 39]. Also, it is not genetically inherited as the rabbits less than two months are unaffected by the virus [29]. This disease caused high rabbit mortality in China (1984), Europe (1988) and Spain (1991) [28, 39]. Based on this, RHD was introduced as a biocontrol agent to control the rabbit pest population in Australia (1993) and New Zealand (1997), which

*Corresponding author

Email addresses: jyoti.guptamaths@gmail.com (Jyoti Gupta), jdhar.iiitmg@gmail.com (Joydip Dhar), sinhapoonam1966@gmail.com (Poonam Sinha)

doi: 10.22436/jmcs.029.03.02

Received: 2021-09-07 *Revised:* 2022-06-16 *Accepted:* 2022-07-04

initially results that rabbit numbers started a decline. However, its long-term effects are a decline in the abundance of healthy red foxes and an increase in alternative prey species [18]. Sarcoptic mange disease also has a considerable impact on the population level in a wide range of species worldwide, specifically grey wolves (Canis lupus lupus), red foxes (Vulpes vulpes), and coyotes (Canis latrans) in the USA, and red foxes in Europe and Australia [2]. It is a highly contagious skin disease of mammals caused by the burrowing mite Sarcoptes scabiei. Mange spreads among red foxes either via direct contact or indirectly via den usage [33].

The dynamics of both the host and the interacting species are widely affected by the infectious disease as it affects the population size. Therefore, many authors studied the spread of infection among either of prey-predator [5, 10, 17, 29, 30, 37, 38]. Recently many researchers also discussed the dynamical properties of the system where both prey-predator are suffering from an infection [7, 13, 14, 20, 27]. It is discussed in [8, 31] that healthy prey is active than the infected one. Some articles [6, 16] discussed models with the disease in the predator population, where the diseased predator is not capable to predate on healthy prey [6]. Some researchers discussed the horizontal transmission of disease from predator to predator [13, 34]. Many mathematicians formulated models discussing the effect of alternative prey species whenever the abundance of predator's primary prey changed [4, 25]. Pech and Hood [28] have done the only quantitative analysis of rabbit-alternative prey-fox dynamics and discussed the consequences of RHD on the red fox population and its alternative prey. Roy and Upadhyay's [29] studied RHD's effect on the European rabbit-red fox spatiotemporal dynamics. This article discussed that the red fox population is declining due to rabbit hemorrhagic disease in its prey, i.e., European rabbit. The article [29] also considered that red fox predates only on rabbits, and alternative food supply is constant or static. Both of these articles [28, 29] have not discussed the effect of mange disease and hunting on the red fox population.

We have inspired from the model [28] and designed a four-compartment spatio-temporal model with European rabbits, alternative prey, healthy red fox, and mange-infected red fox populations. We have done qualitative analysis on rabbit-alternative prey-fox dynamics considering that the population of European rabbits (primary prey) dramatically declines following RHD-induced crashes, and due to scarcity of rabbits, foxes switch their diet to alternative prey. The present model is the more realistic model than [29] as the red fox is a generalist predator, predates on much different prey when rabbits are at low densities [9]. We have also considered mange disease and hunting [40] in the red fox population. This article aims to discuss the conditions for controlling the red fox population despite RHD disease in rabbits and the results of incorporating alternative prey species in rabbit-red fox spatio-temporal dynamics presented by [29].

The following Section 2 contains a four-compartment spatiotemporal model incorporating alternative prey and mange disease in red fox in rabbit-fox dynamics. In Section 3, we have executed the analysis of the eco-epidemiological system without diffusion to expose its biological importance; Subsection 3.1 shows the positivity and boundedness of the solutions of the system. Subsection 3.2 contains different steady-states of the dynamical system following their existing conditions, the mange-reproduction number, and the linear stability analysis of the equilibrium state of the reduced two-compartment model system. Subsection 3.3 investigates the linear stability and bifurcation behavior of the steady-state of the non-spatial four-compartment system following the global stability of the equilibrium state of the same in 3.4. The section 4 contains the analysis of the spatiotemporal model including local stability in Subsection 4.1, Turing instability in Subsection 4.2 and Higher-order stability in Subsection 4.3. In section 5, we have presented a numerical simulation of temporal and spatiotemporal models to verify our analytical findings. We have discussed and concluded the quantitative results in section 6. It also contains the biological interpretation of our analytical findings.

2. The systematic development of the proposed model

We have three types of population: the RHD-infected rabbits (primary prey) denoted by N, the healthy prey (alternative prey) denoted by A, and the predator (red fox). The predator population is divided into two-compartment healthy and mange-infected foxes denoted by P and I, respectively. The proposed model is based on the following assumptions.

Assumption 1. In the absence of a predator population, the rabbit population is growing logistically as $\frac{dN}{dt} = rN(1-\frac{N}{K})$, despite the decline in rabbit abundance due to RHD, where, r is the intrinsic birth rate, and K is the carrying capacity.

Assumption 2. The alternative prey population grows exponentially with a growth rate of b and dies at a natural death rate of μ_1.

Assumption 3. We assume that θ is the total feeding capacity of a healthy fox. The healthy fox predates both rabbit and alternative prey with the linear functional response. The healthy red fox prefers to predate on a rabbit with a predation rate of ω_1. Hence, $\omega_1 N$ part of its total need is fulfilled by the rabbit population. Further, the red fox predates on the alternative prey with a predation rate ω_3. Hence, $\omega_3(\theta - \omega_1 N)$ is the rest of the red fox's total need fulfilled by alternative prey. Here, we choose a linear functional response for healthy foxes as they can easily search for their food despite a decline in the abundance of rabbits [11, 19, 23, 26, 32].

Assumption 4. Mange-infected fox predates only on RHD-infected rabbit population with Holling type-II functional response with $\frac{\omega_2 N}{a+N}$ rabbits per fox at a given point in time. We have used Holling type-II response for mange-infected foxes as they are physically weak and cannot easily search for their food [11, 19, 23, 26, 32]. Due to the same reason, mange-infected red foxes cannot hunt on alternative prey. The mange-infected fox dies with a disease death rate μ_3.

Assumption 5. The conversion coefficients of healthy fox due to consumption of RHD-infected rabbits and alternative prey are e_1 and e_3, respectively. The conversion coefficient of mange-infected fox due to healthy rabbit is e_2.

Assumption 6. Healthy red foxes are susceptible to mange disease and get the infection from mange-infected foxes with a bilinear incidence rate of β. The healthy red dies with a disease death rate μ_2.

Assumption 7. We considered culling or hunting only in mange-infected foxes as they are weak and can easily be hunted. The rate of culling or hunting is h.

Above assumptions lead to the following set of the autonomous non-linear differential equations:

$$\left.\begin{aligned}
\frac{dN}{dt} &= rN\left(1-\frac{N}{K}\right) - \omega_1 NP - \frac{\omega_2 NI}{a+N},\\
\frac{dA}{dt} &= bA - \omega_3\theta\left(1-\frac{\omega_1 N}{\theta}\right)AP - \mu_1 A,\\
\frac{dP}{dt} &= e_1\omega_1 NP + e_3\omega_3\theta\left(1-\frac{\omega_1 N}{\theta}\right)AP - \beta PI - \mu_2 P,\\
\frac{dI}{dt} &= \frac{e_2\omega_2 NI}{a+N} + \beta PI - hI - \mu_3 I,
\end{aligned}\right\} \tag{2.1}$$

with $N(0) = N_0 > 0$, $A(0) = A_0 > 0$, $P(0) = P_0 > 0$, $I(0) = I_0 > 0$, where all the system parameters r, K, ω_1, ω_2, ω_3, b, θ, a, μ_1, μ_2, μ_3, h, e_1, e_2, and e_3 are positive constant. Here, the per capita intrinsic and exponential growth rate of rabbit and alternative prey per day is represented by r and b, respectively. The parameter K is the environment carrying capacity for rabbits per unit area, and β is the mange-infection

rate from susceptible predator to infected predator. The parameters ω_1, ω_2, and ω_3 are the predation rates per predator per day. The predation rate on the rabbit and alternative prey by a susceptible fox is denoted by ω_1 and ω_3, respectively. While ω_2 represents the predation rate of the mange-infected fox on RHD-infected rabbit. The parameter θ represents maximum food intake per fox per unit of time, and a denotes the half-saturation constant, which reduces the infection rate due to spatial or social distribution and time limitation. The death rate for alternative prey and susceptible predator per day is represented by μ_1 and μ_2, respectively. While μ_3 denotes the disease death rate of the mange-infected fox. The parameters e_1 and e_2 are the conversion coefficient of infectious rabbits to susceptible and mange-infected predators per day. While e_3 is the conversion coefficient of alternative prey to susceptible predator per day. The hunting or culling rate per day per unit area caused by human activities stands at h.

The prey and predator migrate to other spatial locations for their basic needs, such as searching for better food, shelter, and mate. So we assume that these populations freely move in x and y directions, which needs to include the diffusion term in the model, revealing that the animal movement is random and uniformly distributed in all directions. The diffusion coefficient for rabbit, alternative prey, healthy fox, and mange-infected fox are D_N, D_A, D_P, and D_I, respectively. Suppose all the population is confined to a fixed bounded domain Ω in R^4_+. We led to consider the following set of reaction-diffusion equations:

$$\left.\begin{aligned}
&\frac{\partial N}{\partial t} - D_N\nabla^2 N = rN\left(1-\frac{N}{K}\right) - \omega_1 NP - \frac{\omega_2 NI}{a+N},\\
&\frac{\partial A}{\partial t} - D_A\nabla^2 A = bA - \omega_3\theta\left(1-\frac{\omega_1 N}{\theta}\right)AP - \mu_1 A,\\
&\frac{\partial P}{\partial t} - D_P\nabla^2 P = e_1\omega_1 NP + e_3\omega_3\theta\left(1-\frac{\omega_1 N}{\theta}\right)AP - \beta PI - \mu_2 P,\\
&\frac{\partial I}{\partial t} - D_I\nabla^2 I = \frac{e_2\omega_2 NI}{a+N} + \beta PI - hI - \mu_3 I.
\end{aligned}\right\} \tag{2.2}$$

The boundary and initial conditions are: $(\mathbf{n}.\nabla)N = (\mathbf{n}.\nabla)A = (\mathbf{n}.\nabla)P = (\mathbf{n}.\nabla)I = 0$, for $z \in \partial\Omega$, $t > 0$, and $N(z,0) = N(0) > 0$, $A(z,0) = A(0) > 0, P(z,0) = P(0) > 0, I(z,0) = I(0) > 0$, where $z = (x,y) \in \Omega = [0,\delta] \times [0,\delta]$. Here, we consider the homogeneous Neumann boundary conditions because the system (2.2) is self-contained, and there is no population flux across the boundary $\partial\Omega$. Further, $\mathbf{n}$ is an outward drawn unit normal vector to the boundary $\partial\Omega$ of the region Ω. It is beneficial to understand the temporal dynamics of a system before analyzing the spatiotemporal system. In the following Section 3, we will analyze the system (2.1).

3. Temporal model

This section analyzes the positivity and boundedness of the system (2.1) to show that the population of interacting species in a particular habitat is always positive and never grows exponentially for a long time due to the limited resources in that area.

3.1. Positivity and boundedness

Theorem 3.1. *The solutions of the system* (2.1) *with initial conditions are positive,* $\forall t \geqslant 0$.

Proof. We write the equations of the system (2.1) for $t \in [0,\tau]$ in the following form:

$$\frac{dN}{dt} \geqslant -r\frac{N^2}{K} - \omega_1 NP - \frac{\omega_2 NI}{a+N},\ \frac{dA}{dt} \geqslant -\omega_3\theta\left(1-\frac{\omega_1 N}{\theta}\right)AP - \mu_1 A,\ \frac{dP}{dt} \geqslant -\beta PI - \mu_2 P,\ \frac{dI}{dt} \geqslant -hI - \mu_3 I.$$

Now, we use theory of differential equation and find out the following solutions:

$$N(t) \geqslant \frac{N(0)}{N(0)\int_0^t \frac{r}{K}dv + \exp\{-\int_0^t(\omega_1 P + \frac{\omega_2 I}{a+N})du\}},\quad A(t) \geqslant A(0)\exp\{-\int_0^t(\omega_3\theta\left(1-\frac{\omega_1 N}{\theta}\right)P + \mu_1)du\},$$

$$P(t) \geqslant P(0)\exp\{-\int_0^t (\beta I + \mu_2)du\}, \qquad I(t) \geqslant I(0)\exp\{-(h+\mu_3)t\}.$$

Similarly, $N(t)$, $A(t)$, $P(t)$ and $Y(t)$ are also positive for the intervals $[\tau, 2\tau] \cdots [n\tau, (n+1)\tau]$, $\forall n \in N$. Hence, by mathematical induction $N(t)$, $A(t)$, $P(t)$ and $Y(t)$ are positive for all $t \geqslant 0$. □

Theorem 3.2. *The non-negative solutions of the system* (2.1) *initiate in* R^4_+ *and uniformly bounded for any initial value.*

Proof. Let us assume that $W(t) = N(t) + A(t) + P(t) + I(t)$, then the rate of change of W is,

$$\frac{dW}{dt} = r\left(1 - \frac{N}{K}\right)N + (e_1 - 1)\omega_1 NP + \frac{(e_2 - 1)\omega_2 NI}{a + N} + bA$$
$$+ (e_3 - 1)\omega_3\theta\left(1 - \frac{\omega_1 erN}{\theta}\right)AP - \mu_1 A - \mu_2 P - hI - \mu_3.$$

Since, $e_1, e_2, e_3 \leqslant 1$, therefore for $\gamma = \min\{r, h + \mu_3, \mu_2, \mu_1 - b\}$, we have obtained:

$$\frac{dW}{dt} + \gamma W \leqslant -\frac{rN^2}{K} + 2rN \Rightarrow 0 \leqslant W(t) \leqslant \frac{rK}{\gamma}(1 - e^{-\gamma t}) + W(0)e^{-\gamma t}.$$

If we take $t \to \infty$, the above expression results $\lim_{t\to\infty} \sup W(t) \leqslant \frac{rK}{\gamma}$. Thus, $W(t) = N(t) + A(t) + P(t) + I(t) \leqslant \frac{rK}{\gamma}$. Hence, all population are uniformly bounded for any initial value in $\Omega = \{(N, A, P, I) \in R^4_+ : N \leqslant \eta_1, A \leqslant \eta_2, P \leqslant \eta_3, I \leqslant \eta_4\}$. □

3.2. The classification and existence of equilibriums

The equilibriums for the proposed system are following.

(a) The trivial equilibrium $E_0(0, 0, 0, 0)$.

(b) The axial equilibrium $E_1(K, 0, 0, 0)$.

(c) The disease-free equilibrium $E_2(0, \bar{A}, \bar{P}, 0)$.

(d) The diseased equilibrium $E_3(\hat{N}, 0, 0, \hat{I})$.

(f) The alternative prey-free without infected predator equilibrium (APFWIPE) $E_4(\dot{N}, 0, \dot{P}, 0)$.

(e) The alternative prey-free infected predator equilibrium (APFIPE) $E_5(\tilde{N}, 0, \tilde{P}, \tilde{I})$.

(f) The mange-free equilibrium (MFE) $E_6(\vec{N}, \vec{A}, \vec{P}, 0)$.

(h) The coexistence equilibrium $E_7(\ddot{N}, \ddot{A}, \ddot{P}, \ddot{I})$.

We have used the Kolmogorov theorem [22, 35] to examine the existence and linear stability of equilibrium of the system (2.1). We partition the system (2.1) into three independent subsystems (3.1), (3.2), and (3.3). The interaction functions of subsystems are continuous, and partial derivatives of these functions are also continuous on the state space R^4_+. Also, the Theorem 3.1 refers that the solutions of these subsystems, which start in the domain Ω, are uniformly bounded. The Kolmogorov theorem assures a stable equilibrium point in the positive quadrant of the phase space under certain conditions [35] and a stable limit cycle behavior if these conditions violate.

Subsystem 1. We obtained the first subsystem in the absence of alternative prey and mange-infected predator as

$$\frac{dN}{dt} = rN\left(1 - \frac{N}{K}\right) - \omega_1 NP, \quad \frac{dP}{dt} = e_1\omega_1 NP - \mu_2 P. \tag{3.1}$$

Subsystem 2. We obtained the second subsystem in the absence of alternative prey and healthy predator as

$$\frac{dN}{dt} = rN\left(1-\frac{N}{K}\right) - \frac{\omega_2 NI}{a+N}, \quad \frac{dI}{dt} = \frac{e_2\omega_2 NI}{a+N} - hI - \mu_3 I. \tag{3.2}$$

Subsystem 3. We obtained the last subsystem in the absence of RHD-infected rabbit and mange-infected predator as

$$\frac{dA}{dt} = bA - \omega_3\theta AP - \mu_1 A, \quad \frac{dP}{dt} = e_3\omega_3\theta AP - \mu_2 P. \tag{3.3}$$

Now, we observe that the subsystem (3.1)-(3.3) is a Kolmogorov system under the conditions, $R_{01} = \frac{e_1\omega_1 K}{\mu_2} > 1$, $R_{02} = \frac{e_2\omega_2 K}{(h+\mu_3)(a+K)} > 1$, and $R_{03} = \frac{\theta e_3\omega_3 K}{\mu_2} > 1$, respectively. We next proceed to find uniform steady states of the Kolmogorov systems (3.1)-(3.3) with these three conditions along with their existence conditions.

3.2.1. *Mange reproduction number*

The basic reproduction number ensures the number of infective cases; one primary case has over its infectious period in an uninfected population. The mange reproduction number is

$$R_{man} = \frac{e_2\omega_2\vec{N} + \beta\vec{P}(a+\vec{N})}{(a+\vec{N})(h+\mu_3)}.$$

3.2.2. *Uniform steady states for the reduced two component systems*

We consider the system (3.1) which has three non-negative steady states: the trivial equilibrium $E_{11}(0,0)$, axial equilibrium $E_{12}(K,0)$, and non-trivial equilibrium $E_{13}(\dot{N},\dot{P})$. The nontrivial equilibrium is given by $\dot{N} = \frac{\mu_2}{e_1\omega_1}$ and $\dot{P} = \frac{r(-\mu_2+e_1\omega_1 K)}{e_1\omega_1^2 K}$. It is clear from the expression of $\dot{P}$ that the uniform steady state E_{13} exists when condition $R_{01} > 1$ holds. Similarly, the steady states of systems (3.2) are $E_{21}(0,0)$, $E_{22}(K,0)$ and $E_{23}(\hat{N},\hat{I})$, where, $\hat{N} = \frac{a(h+\mu_3)}{e_2\omega_2-(h+\mu_3)}$ and $\hat{I} = \frac{are_2(e_2\omega_2 K-(a+K)(h+\mu_3))}{K(h+\mu_3-e_2\omega_3)^2}$. It is clear that, equilibrium $E_{23} = (\hat{N},\hat{I})$ exists provided following conditions are satisfied: $\frac{e_2\omega_2}{(h+\mu_3)} > 1$ and $R_{02} = \frac{e_2\omega_2 K}{(h+\mu_3)(a+K)} > 1$. Lastly, the system (3.3) has steady states $E_{31}(0,0)$ and $E_{32}(\bar{A},\bar{P})$, where, $\bar{A} = \frac{\mu_2}{e_3\omega_3\theta}$ and $\bar{P} = \frac{b-\mu_1}{\theta\omega_3}$. This equilibrium exists when $b > \mu_1$ holds.

3.2.3. *Linear stability of the non-spatial two component NP system*

We proceed to analyze the local stability of the system (3.1). The trivial equilibrium $E_{11}(0,0)$ always exist and the corresponding eigen values are, $\lambda_1 = r > 0$ and $\lambda_2 = -\mu_2$. Clearly, equilibrium E_{11} is a saddle point. The eigenvalues for the predator-free equilibrium $E_{12}(K,0)$ are, $\lambda_1 = -r < 0$ and $\lambda_2 = -\mu_2 + e_1\omega_1 K$. The second eigen value $\lambda_2 < 0$ if and only if $R_{01} = \frac{e_1\omega_1 K}{\mu_2} > 1$. Therefore, equilibrium E_{12} is locally asymptotically stable provided $R_{01} < 1$ holds, otherwise it is a saddle point.

Now, we analyze the stability of the coexistence state $E_{13}(\dot{N},\dot{P})$. The entries for variational matrix $\dot{J}$ for this equilibrium are, $\dot{J_{11}} = r(1-\frac{\mu_2}{e_1 K\omega_1}) - \frac{r\mu_2}{e_1 K\omega_1} - \dot{P}\omega_1$, $\dot{J_{12}} = \frac{-\mu_2}{e_1}$, $\dot{J_{21}} = e_1\omega_1\dot{P}$, $\dot{J_{22}} = 0$. The eigen values related to equilibrium $E_{13}(\dot{N},\dot{P})$ are negative or have negative real parts if and only if $\mathrm{Trac}(\dot{J}) = \lambda_1 + \lambda_2 = \frac{-r\mu_2}{e_1\omega_1 K} < 0$ and $\mathrm{Det}(\dot{J}) = \lambda_1\lambda_2 = r\mu_2(1-\frac{\mu_2}{e_1\omega_1 K}) > 0$, which is possible if and only if $R_{01} > 1$ holds. Hence, if the equilibrium $E_{13}(\dot{N},\dot{P})$ exists, it is locally asymptotically stable in the interior of the positive quadrant of the N-P plane.

3.2.4. Linear stability of the non-spatial two component NI systems

We study the linear stability behavior of the system (3.2) as follows. The eigenvalues associated with the equilibrium $E_{21}(0,0)$ of the system (3.2) are, $\lambda_1 = r > 0$ and $\lambda_2 = -h - \mu_3 < 0$. Therefore, equilibrium E_{21} is saddle point. Similarly, eigenvalues associated with $E_{22}(K,0)$ are, $\lambda_1 = -r < 0$ and $\lambda_2 = -h - \mu_3 + \frac{e_2\omega_2 K}{(a+K)}$. The eigenvalue λ_2 is negative when $R_{02} = \frac{e_2\omega_2 K}{(h+\mu_3)(a+K)} < 1$. Hence, the predator-free equilibrium is locally asymptotically stable $R_{02} < 1$. Finally, the entries of variational matrix $\hat{J}$ for the coexistence equilibrium $E_{23}(\hat{N},\hat{I})$ are $\hat{J_{11}} = r(1-\frac{2\hat{N}}{K}) - \frac{\omega_2 I}{(a+\hat{N})}(1-\frac{\hat{N}}{(a+\hat{N})})$, $\hat{J_{12}} = \frac{-\omega_2\hat{N}}{(a+\hat{N})}$, $\hat{J_{21}} = (1-\frac{\hat{N}}{(a+\hat{N})})\frac{e_2\omega_2\hat{I}}{(a+\hat{N})}$, $\hat{J_{22}} = \frac{e_2\omega_2\hat{N}}{(a+\hat{N})} - h - \mu_3$. Now, the eigenvalues of equilibrium $E_{23}(\hat{N},\hat{I})$ are negative or have negative real parts if and only if $\mathrm{Trac}(\hat{J}) = r(1-\frac{2\hat{N}}{K}) - \frac{\omega_2\hat{I}}{(a+\hat{N})}(1-\frac{\hat{N}}{(a+\hat{N})}) < 0$, and $\mathrm{Det}(\hat{J}) = \frac{b((h+\mu_3)(h+\mu_3-e_2\omega_2)^2)}{ae_2^2\omega_2^2} > 0$, which is always true. Hence, if the coexistence equilibrium $E_{23}(\hat{N},\hat{I})$ exists, it is locally asymptotically stable in the interior of the positive quadrant of the N-I plane.

3.2.5. Linear stability of the non-spatial two component AP systems

Finally, we consider the local stability of the subsystem (3.3). The eigenvalues associated with the equilibrium $E_{31}(0,0)$ are $\lambda_1 = b - \mu_1 > 0$ and $\lambda_2 = -\mu_2 < 0$. Clearly, this is a saddle point as $b > \mu_1$ always holds for the existence of the system (3.3). Again, the eigenvalues related with equilibrium $E_{32}(\bar{A},\bar{P})$ are $\lambda_1, \lambda_2 = \pm\sqrt{\mu_2(\mu_1 - b)}$. It is clear from the expression that these eigenvalues are imaginary. Hence, the equilibrium E_{32} exists, but unstable in the interior of the positive quadrant of A-P plane.

3.2.6. Existence of APFIPE, MFE, and interior equilibrium

In the absence of an alternative prey population, we find the following values of I and P from the last two equations of the system (2.1):

$$I = \frac{e_1\omega_1 N - \mu_2}{\beta}, \quad P = \frac{(a+N)(h+\mu_3) - e_2\omega_2 N}{\beta(a+N)}.$$

We substitute these value to first equation of system (2.1) and obtain the following nonlinear algebraic equation:

$$Q_2N^2 + Q_1N + Q_0 = 0, \tag{3.4}$$

where, $Q_2 = r\beta$, $Q_1 = (ar\beta(a-K) + K\omega_1(e_1\omega_2 - e_2\omega_2 + (h+\mu_3))$, $Q_0 = aK(\omega_1(h+\mu_3) - r\beta) - K\mu_2\omega_2$. It is clear that quadratic equation (3.4) has exactly one positive root if and only if $Q_0 < 0$. After calculating the value of N, we can easily calculate the value of I and P. In addition to this, I and P are positive if $R_{01} > 1$ and $R_{02} < 1$ hold, respectively. This complete the existence of equilibrium $E_5(\tilde{N},0,\tilde{P},\tilde{I})$. In the absence of a mange-infected predator population, we find the following values of A and P from the first and third equation of the system (2.1):

$$A = \frac{\mu_2 - e_1\omega_1 N}{e_3\omega_3(\theta - N\omega_1)}, \quad P = \frac{r(K-N)}{K\omega_1}.$$

We substitute these value to second equation of system (2.1) and obtain the following nonlinear algebraic equation:

$$T_2N^2 + T_1N + T_0 = 0, \tag{3.5}$$

where, $T_2 = r\omega_1\omega_3$, $T_1 = -Kr\omega_1\omega_3 - \theta r\omega_3$, $T_0 = K\omega_1(\mu_1 - b) + \theta Kr\omega_3$. It is clear that quadratic equation (3.5) has exactly one positive root if and only if $T_0 < 0$. After calculating the value of N, we can easily calculate the value of A and P. Further, A is positive if $R_{01} < 1$ holds. Hence, the equilibrium $E_6(\vec{N},\vec{A},\vec{P},0)$ exists when $(\dot{N},\dot{P})$ is unstable. This complete the existence of equilibrium $E_6(\vec{N},\vec{A},\vec{P},0)$. Finally, we investigate the existence conditions of the coexistence equilibrium $E_7(\ddot{N},\ddot{A},\ddot{P},\ddot{I})$, which can be obtained

from the solution of system of differential equation (2.1). We solve the first, third and fourth equations of system (2.1) and obtained the following values:

$$P = \frac{a(h+\mu_3) + N((h+\mu_3) - e_2\omega_3)}{\beta(a+N)}, \tag{3.6}$$

$$I = \frac{r\beta(K-N)(a+N) - \omega_1 K((h+\mu_3)(a+N) - e_2\omega_2 N)}{\omega_2 K}, \tag{3.7}$$

$$A = \frac{(\mu_2 - e_1\omega_1 N)\omega_2 K + \beta(r\beta(K-N)(a+N) - \omega_1 K((h+\mu_3)(a+N) - e_2\omega_2 N))}{\omega_1\omega_2 e_3 K(\theta - \omega_1 N)}. \tag{3.8}$$

Now, if we substitute value of P in the second equation of system (2.1), we get a nonlinear algebraic polynomial in N.

$$V_2 N^2 + V_1 N + V_0 = 0, \tag{3.9}$$

where, $V_2 = \omega_1\omega_3((h+\mu_3) - e_2\omega_2), V_1 = \beta(b-\mu_1) + \omega_3\theta(e_2\omega_2 - (h+\mu_3)) + a\omega_1\omega_3(h+\mu_3)$, $V_0 = a(\beta(b-\mu_1) - \theta\omega_3(h+\mu_3))$. It is clear from the expressions that there is only one sign change in (3.9) if and only if $R_{02} < 1$ and $V_0 < 0$. In this situation the equation (3.9) has only one positive real solution. After having value of N, we can easily find the value of A, P and I from expressions (3.6), (3.7), and (3.8), respectively. This completes the existence of coexistence equilibrium $E_7(\ddot{N}, \ddot{A}, \ddot{P}, \ddot{I})$.

3.3. *Linear stability and bifurcation analysis*

In this section, we investigate the local stability behavior of the system (2.1) around each of the equilibrium points, E_0-E_7.

Theorem 3.3. *The trivial equilibrium* $E_0(0,0,0,0)$ *is saddle point.*

Proof. The eigenvalues λ_N, λ_A, λ_P, λ_I associated with the equilibrium E_0 are r, $b-\mu_1$, $-\mu_2$, $-h-\mu_3$. Therefore, equilibrium E_0 is a saddle point. □

Theorem 3.4. *The axial equilibrium* $E_1(K,0,0,0)$ *is locally asymptotically stable if conditions* $R_{01} < 1$ *and* $R_{02} < 1$ *hold.*

Proof. The eigenvalues, λ_N, λ_A, λ_P, λ_I associated with the E_1 are, $-r$, $b-\mu_1$, $-\mu_2 + e_1\omega_1 K$, $-h-\mu_3 + \frac{e_2\omega_2 K}{(a+K)}$, respectively. We know that $\lambda_A = b - \mu_1 < 0$ must be hold for the existence of equilibrium E_1 otherwise alternative prey population will be positive. Again, $\lambda_P = -\mu_2 + e_1\omega_1 K < 0$, when $R_{01} < 1$ and $\lambda_I = -h - \mu_3 + \frac{e_2\omega_2 K}{a+K} < 0$ when $R_{02} < 1$. Hence, equilibrium state E_1 is locally asymptotically stable when equilibrium E_2, E_3 and E_4 are locally unstable. □

Theorem 3.5. *The disease-free equilibrium* $E_2(0,\bar{A},\bar{P},0)$ *is always unstable.*

Proof. The stability properties of equilibrium $E_2(0,\bar{A},\bar{P},0)$ depend on stability properties of E_{32}. We can clearly see from (3.2.5) that the equilibrium E_{32} is always unstable. Hence, disease-free equilibrium $E_2(0,\bar{A},\bar{P},0)$ is always unstable. □

Theorem 3.6. *The diseased equilibrium* $E_3(\hat{N},0,0,\hat{I})$ *is locally asymptotically stable if* $R_{02} > 1$, $\lambda_A < 0$ *and* $\lambda_P < 0$ *holds, where,* $\lambda_A < 0$ *and* $\lambda_P < 0$ *are given in the proof.*

Proof. The entries for variational matrix $J(E_3)$ for the equilibrium E_3 are, $a_{11} = \frac{-r\hat{N}}{K} + r(1-\frac{\hat{N}}{K}) - \frac{\omega_2\hat{I}}{a+\hat{N}} + \frac{\omega_2\hat{N}\hat{I}}{(a+\hat{N})^2}$, $a_{12} = 0$, $a_{13} = -\omega_1\hat{N}$, $a_{14} = \frac{-\omega_2\hat{N}}{(a+\hat{N})}$, $a_{21} = 0$, $a_{22} = b-\mu_1$, $a_{23} = 0$, $a_{24} = 0$, $a_{31} = 0$, $a_{32} = 0$, $a_{33} = -\mu_2 + e_1\omega_1\dot{N} - \beta\hat{I}$, $a_{34} = 0$, $a_{41} = \frac{-e_2\omega_2\hat{N}\hat{I}}{(a+\hat{N})^2} + \frac{e_2\omega_2\hat{I}}{(a+\hat{N})}$, $a_{42} = 0$, $a_{43} = \beta\hat{I}$, $a_{44} = -h-\mu_3 + \frac{e_2\omega_2\hat{N}}{a+\hat{N}}$. The stability properties of the equilibrium $E_3(\hat{N},0,0,\hat{I})$ are similar as stability properties of equilibrium

$(\hat{N}, \hat{I})$ in the interior of positive quadrant of NI-plane. Moreover, its properties depend on whether the associated eigenvalues are positive or negative. It follows from (3.2.4) that the eigenvalues λ_N and λ_I are either negative or have negative real parts if $R_{02} > 1$ holds, while the eigenvalues λ_A and λ_P will be negative if and only if, $\lambda_A = b - \mu_1 < 0$, $\lambda_P = -\mu_2 + e_1\omega_1\hat{N} - \beta\hat{I} < 0$. Hence, equilibrium state $E_2(\hat{N}, 0, 0, \hat{I})$ is locally asymptotically stable provided $\lambda_A < 0$ and $\lambda_P < 0$. Therefore diseased equilibrium is locally stable.. □

Theorem 3.7. *The equilibrium* APFWIPE, *i.e.,* $E_4(\dot{N}, 0, \dot{P}, 0)$ *is locally asymptotically stable when* $R_{01} > 1$, $R_{man} < 1$, *and* $\lambda_A < 0$, *where,* $\lambda_A < 0$ *is given in the proof.*

Proof. The entries of variational matrix $J(E_4)$ are, $b_{11} = \frac{-r\dot{N}}{K} + r(1 - \frac{\dot{N}}{K}) - \omega_1\dot{P}$, $b_{12} = 0$, $b_{13} = -\omega_1\dot{N}$, $b_{14} = \frac{-\omega_2\dot{N}}{(a+\dot{N})}$, $b_{21} = 0$, $b_{22} = b - \mu_1 - \theta\omega_3\dot{P}(1 - \frac{\omega_1\dot{N}}{\theta})$, $b_{23} = 0$, $b_{24} = 0$, $b_{31} = e_1\omega_1\dot{P}$, $b_{32} = \theta e_3\omega_3\dot{P}(1 - \frac{\omega_1}{\theta})$, $b_{33} = -\mu_2 + e_1\omega_1\dot{N}$, $b_{34} = -\beta\dot{P}$, $b_{41} = 0$, $b_{42} = 0$, $b_{43} = 0$, $b_{44} = -h - \beta\dot{P} - \mu_3 + \frac{e_2\omega_2\dot{P}}{a+\dot{N}}$. The stability properties of APFWIPE, i.e., $E_2(\dot{N}, 0, \dot{P}, 0)$ are similar as stability properties of equilibrium $(\dot{N}, \dot{P})$ in the interior of positive quadrant of N-P plane. It follows from (3.2.3) that the eigen values λ_N and λ_P are either negative or have negative real parts if $R_{01} > 1$ holds. The expressions for eigenvalue λ_A and λ_I are,

$$\lambda_A = b - \mu_1 - \theta\omega_3\dot{P}(1 - \frac{\omega_1\dot{N}}{\theta}),\ \lambda_I = -h + \beta\dot{P} - \mu_3 + \frac{e_2\omega_2\dot{N}}{a + \dot{N}}. \tag{3.10}$$

In the expression (3.10) $\lambda_I < 0$ when $R_{man} < 1$. Hence, equilibrium $E_2(\dot{N}, 0, \dot{P}, 0)$ is locally asymptotically stable provided $R_{01} > 1$, $\lambda_A < 0$ and $R_{man} < 1$. □

Lemma 3.8 ([29, Lemma 1])**.** *Suppose* $J^* = (b_{ij})_{4\times 4}$ *be a matrix with real entries. For* J^* *to be stable, it is necessary and sufficient that*

1. $(-1)^4 \det(J^*) > 0$; *and*
2. $\mu(J^{[2]}) < 0$ *for some Lozinski measure* μ *on* $M_N(T)$, $N = \begin{pmatrix} 3 \\ 2 \end{pmatrix}$; *where* $M_N(T)$ *be the linear space of* 3×3 *matrices with entries in T, where T is either the field of real numbers or complex numbers.*

Lemma 3.9 ([29, Lemma 2])**.** *Let* $J^{[2]} \in M_N(T)$ *be an* $n \times n$ *matrix and let* $\sigma(J^{[2]})$ *be its spectrum. The stability modulus of* $J^{[2]}$ *is* $s(J^{[2]}) = \max\{-\mathrm{Re}\lambda : \lambda \in \sigma(J^{[2]})\}$, *then* $s(J^{[2]}) < 0 \Leftrightarrow \mu(J^{[2]}) < 0$ *for some Lozinski measure* μ *on* $M_N(T)$.

Theorem 3.10. *The equilibrium* APFIPE, $E_5(\tilde{N}, 0, \tilde{P}, \tilde{I})$ *of the system* (2.1) *is locally asymptotically stable if the following condition holds:*

$$(-\beta\tilde{I} - \mu_2 + e_1\tilde{N}\omega_1)(-h + \tilde{P}\beta - \mu_3) + \beta^2\tilde{P}\tilde{I} - e_2\omega_1\beta\tilde{P}\tilde{N}) > 0, \tag{3.11}$$

$$b + r + \frac{\tilde{N}(a + \tilde{N} + \tilde{I})\omega_2}{(a + \tilde{N})^2} + \omega_1\omega_3\tilde{P}\tilde{N} < \frac{2r\tilde{N}}{K} + \mu_1 + \omega_1\tilde{P} + \frac{\omega_2\tilde{X}}{a + \tilde{N}} + \theta\omega_3\tilde{P} < 0, \tag{3.12}$$

$$r + \frac{\omega_2(a + \tilde{N} + \tilde{I})\tilde{N}}{(a + \tilde{N})^2} + e_3\theta\omega_3\tilde{N} < \frac{2r\tilde{N}}{K} + (\frac{\beta\tilde{N}}{\tilde{I}} + \omega_1)\tilde{P} + \frac{\omega_2\tilde{I}}{a + \tilde{N}} + e_3\omega_1\omega_3\tilde{N}^2, \tag{3.13}$$

$$r + \frac{\beta\tilde{I}^2}{\tilde{N}} < \frac{2r\tilde{N}}{K} + \omega_1(\tilde{P} + \tilde{I}) + \frac{a\omega_2\tilde{I}}{(a + \tilde{S})^2}, \tag{3.14}$$

$$b < \mu_1 + (\beta + e_1\omega_1 + \theta\omega_3 - \omega_1\omega_3\tilde{N})\tilde{P}, \tag{3.15}$$

$$b + (\beta - \frac{ae_2\omega_2}{(a + \tilde{N})^2})\tilde{I} + \omega_1\omega_3\tilde{P}\tilde{N} < \mu_1 + \theta\omega_3\tilde{P}, \tag{3.16}$$

$$\frac{e_1\omega_1\tilde{P}\tilde{N}}{\tilde{I}} + e_3\omega_3(\theta - S\omega_1)\tilde{N} < \frac{ae_2\omega_2\tilde{I}}{(a + \tilde{N})^2}. \tag{3.17}$$

Proof. We will proof the local asymptotic stability of $E_5(\tilde{N}, 0, \tilde{P}, \tilde{I})$ using method of first approximation [30]. Further, we use Lemmas 3.8 and 3.9 to proof that equilibrium E_5 is locally stable if $\det[J(E_5)] > 0$ and the Lozinskii measure of the second additive compound matrix of $J(E_5)$ is negative. The entries of jacobian $J(E_5)$ are, $e_{11} = -\frac{r\tilde{N}}{K} + r\left(1 - \frac{\tilde{N}}{K}\right) - \omega_1\tilde{P} + \frac{\omega_2\tilde{N}\tilde{I}}{(a+\tilde{N})^2} - \frac{\omega_2\tilde{I}}{a+\tilde{N}}$, $e_{12} = 0$, $e_{13} = -\omega_1\tilde{N}$, $e_{14} = -\frac{\omega_2\tilde{N}}{a+\tilde{N}}$, $e_{21} = 0$, $e_{22} = b - \mu_1 - \theta\tilde{P}(1 - \frac{\omega_1\tilde{N}}{\theta})\omega_3$, $e_{23} = 0$, $e_{24} = 0$, $e_{31} = e_1\tilde{P}\omega_1$, $e_{32} = e_3\theta\tilde{P}(1 - \frac{\tilde{N}\omega_1}{\theta})\omega_3$, $e_{33} = -\beta\tilde{I} - \mu_2 + e_1\omega_1\tilde{N}$, $e_{34} = -\beta\tilde{P}$, $e_{41} = -\frac{e_2\omega_2\tilde{N}\tilde{I}}{(a+\tilde{N})^2} + \frac{e_2\omega_2\tilde{I}}{a+\tilde{N}}$, $e_{42} = 0$, $e_{43} = \beta\tilde{I}$, $e_{44} = -h + \tilde{P}\beta - \mu_3 + \frac{e_2\tilde{N}\omega_2}{a+\tilde{N}}$. The expression $\det[J(E_5)]$ is given as:

$$\left(\left(-\frac{r\tilde{N}}{K} + r\left(1 - \frac{\tilde{N}}{K}\right) - \tilde{P}\omega_1\right)\left((-\beta\tilde{I} - \mu_2 + e_1\tilde{N}\omega_1)\left(-h + \beta\tilde{P} - \mu_3 + \frac{e_2\omega_2\tilde{N}}{a+\tilde{N}}\right) + \beta^2\tilde{P}\tilde{I}\right)\right.$$
$$\left. + \left(\frac{\omega_2\tilde{N}\tilde{I}}{(a+\tilde{N})^2} - \frac{\omega_2\tilde{I}}{a+\tilde{N}}\right)\left((-\beta\tilde{I} - \mu_2 + e_1\omega_1\tilde{N})(-h + \beta\tilde{P} - \mu_3) + \beta^2\tilde{P}\tilde{I} - e_2\omega_1\beta\tilde{P}\tilde{N}\right)\right)\mathcal{D}.$$

Here, $\mathcal{D} = \left(b - \mu_1 - P\theta\left(1 - \frac{\omega_1\tilde{N}}{\theta}\right)\omega_3\right)$. Now, the expression of $\det[J(E_5)]$ is positive when the condition (3.11) holds. The second additive compound matrix of $[J(E_5)]$ is,

$$J^{[2]}(E_5) = \begin{pmatrix} e_{11}+e_{22} & e_{23} & e_{24} & -e_{13} & e_{14} & 0 \\ e_{32} & e_{11}+e_{33} & e_{34} & e_{12} & 0 & -e_{14} \\ e_{42} & e_{43} & e_{11}+e_{44} & 0 & e_{12} & -e_{13} \\ -e_{31} & e_{21} & 0 & e_{22}+e_{33} & e_{34} & -e_{24} \\ -e_{41} & e_{21} & -e_{42} & e_{43} & e_{22}+e_{44} & e_{23} \\ 0 & -e_{41} & e_{31} & -e_{42} & e_{32} & e_{33}+e_{44} \end{pmatrix}.$$

Now, we assume $D = \mathrm{diag}(\tilde{P}, \tilde{N}, \tilde{I}, \tilde{P}, \tilde{P}, \tilde{N})$ and find following the matrix:

$$DJ^{[2]}D^{-1} = \begin{pmatrix} e_{11}+e_{22} & 0 & 0 & -e_{13} & e_{14} & 0 \\ \frac{e_{32}\tilde{N}}{\tilde{P}} & e_{11}+e_{33} & \frac{e_{34}\tilde{N}}{\tilde{P}} & 0 & 0 & -e_{14} \\ 0 & \frac{e_{43}\tilde{I}}{\tilde{N}} & e_{11}+e_{44} & 0 & 0 & \frac{e_{13}\tilde{I}}{\tilde{N}} \\ -e_{31} & 0 & 0 & e_{22}+e_{33} & e_{34} & 0 \\ -e_{41} & 0 & 0 & e_{43} & e_{22}+e_{44} & 0 \\ 0 & -e_{41} & \frac{e_{31}\tilde{N}}{\tilde{I}} & 0 & \frac{e_{32}\tilde{N}}{\tilde{P}} & e_{33}+e_{44} \end{pmatrix}.$$

The above matrix is similar to the matrix $J^{[2]}(E_5)$. Clearly, its stability properties are same as that of $J^{[2]}(E_5)$. According to Gershgorini theorem [24, 29], eigenvalues of the dominant diagonal matrix are negative if all its diagonal elements are negative. After taking $e_{44} = 0$ and $e_{33} = 0$ and, applying matrix row operation the $DJ^{[2]}D^{-1}$ takes the following form:

$$DJ^{[2]}D^{-1} = \begin{pmatrix} e_{11}+e_{22} & 0 & 0 & -e_{13} & e_{14} & 0 \\ \frac{e_{32}\tilde{N}}{\tilde{P}} & e_{11} & \frac{e_{34}\tilde{N}}{\tilde{P}} & 0 & 0 & -e_{14} \\ 0 & \frac{e_{43}\tilde{I}}{\tilde{N}} & e_{11} & 0 & 0 & \frac{e_{13}\tilde{I}}{\tilde{N}} \\ -e_{31} & 0 & 0 & e_{22} & e_{34} & 0 \\ -e_{41} & 0 & 0 & e_{43} & e_{22} & 0 \\ 0 & -e_{41}+\frac{e_{43}\tilde{I}}{\tilde{N}} & \frac{e_{31}\tilde{N}}{\tilde{I}}+e_{11} & 0 & \frac{e_{32}\tilde{N}}{\tilde{P}} & \frac{e_{13}\tilde{I}}{\tilde{N}} \end{pmatrix}.$$

Since, the diagonal elements of the above matrix are negative. Therefore, the matrix is diagonally dominant if it follows the conditions (3.11)-(3.17). This shows that all eigenvalues of matrix $J^{[2]}(E_5)$ are negative, entailing all eigenvalues of matrix $J(E_5)$ are negative. Hence, the equilibrium E_5 is locally asymptotically stable. □

Theorem 3.11. *The* MFE *equilibrium* $E_6(\vec{N}, \vec{A}, \vec{P}, 0)$ *of the system* (2.1) *is locally asymptotically stable if* $R_{man} < 1$ *and* $b - \mu_1 - \omega_3\theta\left(1 - \frac{\omega_1\vec{N}}{\theta}\right)\vec{P} = 0$.

Proof. The entries of jacobian $J(E_6)$ of the system are, $f_{11} = -\frac{r\vec{N}}{K} + r\left(1 - \frac{\vec{N}}{K}\right) - \omega_1\vec{P}$, $f_{12} = 0$, $f_{13} = -\omega_1\vec{N}$, $f_{14} = -\frac{\omega_2\vec{N}}{a+\vec{N}}$, $f_{21} = \omega_1\omega_3\vec{A}\vec{P}$, $f_{22} = b - \mu_1 - \omega_3\theta\left(1 - \frac{\omega_1\vec{N}}{\theta}\right)\vec{P}$, $f_{23} = -\omega_3\theta\left(1 - \frac{\omega_1\vec{N}}{\theta}\right)\vec{A}$, $j_{24} = 0$, $f_{31} = e_1\omega_1\vec{P} - e_3\omega_1\omega_3\vec{P}$, $f_{32} = e_3\omega_3\theta\left(1 - \frac{\omega_1\vec{N}}{\theta}\right)\vec{P}$, $f_{33} = -\mu_2 + e_1\omega_1\vec{N} + e_3\omega_3\theta(1 - \frac{\omega_1\vec{N}}{\theta})\vec{A}$, $f_{34} = -\beta\vec{N}$, $f_{41} = 0$, $f_{42} = 0$, $f_{43} = 0$, $f_{44} = -h + \beta\vec{P} - \mu_3 + \frac{e_2\omega_2\vec{N}}{a+\vec{N}}$. Now, we see that when $f_{22} = 0$, $\det(J(E_6)) = -f_{32}f_{44}(f_{11}f_{23} - f_{21}f_{13})$. Thus, all eigenvalues of $J(E_6)$ are negative if and only if every factor of $\det(J(E_6))$ is negative. We know that $R_{man} < 1$ for mange-free equilibrium. Hence, f_{44} is negative. Further, since f_{32} is always a positive quantity, $-f_{32}$ is negative. Finally, the expressions of f_{11}, f_{23}, f_{21} and f_{13} show that last factor$(f_{11}f_{23} - f_{21}f_{13})$ is also negative. Thus, all eigen values related to the jacobean $J(E_6)$ are negative. Hence, mange-free equilibrium E_6 is stable if $R_{man} < 1$ and $f_{22} = 0$. □

Theorem 3.12. *The interior equilibrium* $E_7(\ddot{N}, \ddot{A}, \ddot{P}, \ddot{I})$ *of system* (2.1) *is locally asymptotically stable if following conditions hold:*

(1) $c_{11} + 2c_{22} + 2c_{33} + 2c_{44} < 0$;

(2) $\frac{c_{11}}{c_{13}} < \frac{c_{41}}{c_{43}} < \min\{\frac{c_{21}}{c_{23}}, \frac{c_{31}}{c_{33}}\}$;

(3) $\frac{c_{41}}{c_{11}} < \frac{c_{44}}{c_{14}} < \frac{c_{43}}{c_{13}}$;

(4) $c_{21} > \max\{\frac{c_{31}c_{44}}{c_{32}}, \frac{c_{11}c_{23}}{c_{32}}\}$;

(5) $c_{23}c_{32} > \max\{\frac{c_{13}c_{34}c_{41}}{c_{44}}, c_{22}c_{33} + c_{11}(c_{22} + c_{33}) + c_{11}^2\}$;

(6) $-\{c_{34}c_{43} + c_{11}c_{44} - c_{11}^2 - c_{44}(c_{22} + c_{33})\} < c_{14}c_{41} < c_{13}c_{31} - c_{11}c_{33}$;

(7) $\max\{\frac{-c_{43}(c_{14}c_{31}+c_{33}c_{34})}{c_{14}c_{41}}\} < c_{11} < \min\{-\frac{(c_{22}c_{33})}{2c_{44}}, \frac{-(c_{22}+c_{33})}{2}\}$;

(8) $c_{21}c_{32} + c_{31}c_{33} + c_{34}c_{41} < 0$.

Proof. The entries of variational matrix $J(E_7)$ are, $c_{11} = \frac{-r\ddot{N}}{K} + r(1 - \frac{\ddot{N}}{K}) - \omega_1\ddot{P} - \frac{\omega_2\ddot{I}}{a+\ddot{N}} + \frac{\omega_2\ddot{N}\ddot{I}}{(a+\ddot{N})^2}$, $c_{12} = 0$, $c_{13} = -\omega_1\ddot{N}$, $c_{14} = \frac{-\omega_2\ddot{N}}{(a+\ddot{N})}$, $c_{21} = 0$, $c_{22} = b - \mu_1 - \theta\omega_3\ddot{P}(1 - \frac{\omega_1\ddot{N}}{\theta})$, $c_{23} = -\theta\omega_3\ddot{A}(1 - \frac{\omega_1\ddot{N}}{\theta})$, $c_{24} = 0$, $c_{31} = e_1\omega_1\ddot{P} - e_3\omega_1\omega_3\ddot{A}\ddot{P}$, $c_{32} = \theta e_3\omega_3\ddot{P}(1 - \frac{\omega_1}{\theta})$, $c_{33} = -\mu_2 + e_1\omega_1\ddot{N} - \beta\ddot{I} - \theta e_3\omega_3(1 - \frac{\omega_1\ddot{N}}{\theta})\ddot{A}$, $c_{34} = -\beta\ddot{P}$, $c_{41} = \frac{-e_2\omega_2\ddot{N}\ddot{I}}{(a+\ddot{N})^2} + \frac{e_2\omega_2\ddot{I}}{(a+\ddot{N})}$, $c_{42} = 0$, $c_{43} = \beta\ddot{I}$, $c_{44} = -h - \beta\ddot{P} - \mu_3 + \frac{e_2\omega_2\ddot{N}}{a+\ddot{N}}$. We write the characteristic equation for $J(E_7)$ as follows:

$$\lambda^4 + B_1\lambda^3 + B_2\lambda^2 + B_3\lambda + B_4 = 0. \tag{3.18}$$

Here,

$$\begin{aligned}
B_1 &= -c_{11} - c_{22} - c_{33} - c_{44},\\
B_2 &= c_{11}(c_{22} + c_{33} + c_{44}) - c_{13}c_{31} - c_{23}c_{32} + c_{22}(c_{33} + c_{44}) - c_{14}c_{41} - c_{34}c_{43} + c_{33}c_{44},\\
B_3 &= c_{22}(c_{13}c_{31} - c_{11}c_{33} - c_{14}c_{41}) + c_{13}(c_{31}c_{44} - c_{21}c_{32}) + c_{11}(c_{23}c_{32} - c_{22}c_{44}) + c_{14}(c_{41}c_{33} - c_{31}c_{43})\\
&\quad + (c_{11} + c_{22})(c_{34}c_{43} - c_{33}c_{44}) + (c_{23}c_{32}c_{44} - c_{13}c_{34}c_{41}),\\
B_4 &= c_{14}c_{32}(c_{23}c_{41} - c_{21}c_{43}) + c_{22}c_{33}(c_{11}c_{44} - c_{41}c_{14}) + c_{22}c_{31}(c_{14}c_{43} - c_{13}c_{44})\\
&\quad + c_{44}c_{32}(c_{13}c_{21} - c_{11}c_{23}) + c_{22}c_{34}(c_{41}c_{13} - c_{11}c_{43}),\\
B_1B_2 - B_3 &= (c_{22} + c_{33})(c_{23}c_{32} - c_{22}c_{33} - c_{11}^2 - c_{11}(c_{22} + c_{33})) - (c_{22} + c_{33})(c_{44}(c_{22} + c_{33}) + 2c_{11}c_{44})\\
&\quad + c_{44}(c_{14}c_{41} + c_{34}c_{43} - c_{11}c_{44} - c_{11}^2 - c_{44}(c_{22} + c_{33})) + c_{13}(c_{21}c_{32} + c_{31}c_{33} + c_{34}c_{41})
\end{aligned}$$

$$+ c_{11}c_{14}c_{41} + c_{14}c_{31}c_{43} + c_{33}c_{34}c_{43}.$$

We can see from the expression of c_{11}, c_{22}, c_{33} and c_{44} that $c_{11} < 0$, $c_{22} > 0$, $c_{33} > 0$ and $c_{44} > 0$. Therefore, to make B_1 positive, condition (1) of this theorem must be followed. Further, the first term and second term of B_3 are positive if the conditions (6) and (4) hold, respectively. The third term is always positive as c_{11} and c_{23} are negative expressions. Finally, fourth and last term of B_3 are positive if conditions (2) and (5) of this theorem hold, respectively. Hence, B_3 is positive if the conditions (2) and (4)-(6) holds. Again, the first and last term of B_4 is positive when it follows condition (2), the second and third term is positive when it follows condition (3) and fourth term is positive when condition (4) hold, and hence B_4 is positive if the conditions (2)-(4) of this theorem hold. Now, the conditions (5)-(8) assure that all terms of $B_1B_2 - B_3$ are positive. □

Example 3.13. For the following set of parameter value: $r = 6.1$, $K = 100$, $\omega_1 = 0.01$, $\omega_2 = 0.75$, $\omega_3 = 0.5$, $\theta = 1.42$, $\mu_1 = 0.6$, $\mu_2 = 0.2$, $\mu_3 = 2$, $\beta = 0.225$, $h = 0.1$, $e_1 = 0.9$, $e_2 = 0.6$, $e_3 = 0.2$, $a = 40$, $b = 5$, the positive equilibrium $E_7(36.907, 825.297, 8.374, 386.067)$ exists and satisfies the Routh-Hurwitz criterion, $B_1 = 0.444577 > 0$, $B_2 = 543.182 > 0$, $B_3 = 39.1236$, $B_4 = 1112.03$, $B_1B_2B_3 - B_1^2B_4 + B_3^2 = 7697.36 > 0$ and $B_1B_2 - B_3 = 202.363 > 0$. Therefore, the system (2.1) is locally asymptotically stable at E_7, if conditions (1)-(8) hold.

3.3.1. Bifurcation analysis

Now, we will study the bifurcation behavior of the system (2.1). We observed that system (2.1) exhibits Hopf bifurcation around coexistence equilibrium E_7 for critical value of hunting rate $h = h_c$ because at this value the equation (3.18) have at least one positive real root or complex conjugate roots with positive real part. At $h = h_c$, the necessary condition for existence of Hopf bifurcation are: $B_1 > 0$, $B_3 > 0$, $B_4 > 0$, $B_1B_2 - B_3 > 0$, $B_1B_2B_3 - B_1^2B_4 - B_3^2 = 0$, and $[\mathrm{Re}\frac{d\omega}{dh}]_{h=h_c} \neq 0$. We considered that $\lambda_n = \omega_n + i\nu_n$ are the roots of equation (3.18) for $n = 1, 2, 3, 4$. We put $\lambda = \omega + i\nu$ in (3.18), compare the real and imaginary parts of resulting equation equal to zero, and eliminate ν between them. We get the following equation in ω:

$$\begin{aligned} 64\omega^6 + 48(B_1 + B_3)\omega^5 + 16(2B_2 + 3B_1B_3)\omega^4 - (B_1^3 - 8B_1B_2 - 9B_1^2B_3 - 24B_2B_3)\omega^3 + 2(B_2(B_1^2 + 2B_2) \\ + B_1(-4 + 3B_2)B_3 + 6B_3^2 - 16B_4)\omega^2 - B_1(-2B_2^2 + (B_1 - 3B_3)B_3)\omega + B_1B_2B_3 - B_1^2B_4 - B_3^2 = 0. \end{aligned} \tag{3.19}$$

The equation (3.19) results $\omega(h_c) = 0$ as $B_1B_2B_3 - B_1^2B_4 - B_3^2 = 0$. Now, on differentiating (3.19) with respect to h and calculate value of derivative for $\omega(h_c) = 0$, we have:

$$\left(\frac{d\omega}{dh}\right)_{h=h_c} = \frac{\frac{d}{dh}(B_1B_2B_3 - B_1^2B_4 - B_3^2)}{(8B_1B_4 - 2B_1B_2^2 + B_1^2B_3 - 3B_3^2B_1)} \neq 0.$$

Thus, the transversity condition holds. This ensures that system (2.1) exhibits Hopf bifurcation at $h = h_c$ shown in the Fig. 6.

3.4. Global stability

Theorem 3.14. *If the equilibrium $E_7(\ddot{N}, \ddot{A}, \ddot{P}, \ddot{I})$ of the system (2.1) is locally asymptotically stable, then it is also globally stable in the interior of the positive region R_+^4 provided following conditions hold:*

$$\frac{1}{e_3} > k_1 > k_2 \ \textit{and} \ \omega_1\ddot{P} < \min\{\frac{2}{\omega_3}\left(\frac{r}{K} - \frac{\omega_2\ddot{I}}{a + \ddot{N}}\right), (1 - K_1e_3)(\theta - \omega_1\ddot{N})\}. \tag{3.20}$$

Proof. We consider the following positive definite Lyapunov function around the equilibrium E_7:

$$V(t) = [N(t) - \ddot{N} - \ddot{N}\frac{N(t)}{\ddot{N}}] + [A(t) - \ddot{A} - \ddot{A}\frac{A(t)}{\ddot{A}}] + k_1[P(t) - \ddot{P} - \ddot{P}\frac{P(t)}{\ddot{P}}] + k_2[I(t) - \ddot{I} - \ddot{I}\frac{I(t)}{\ddot{I}}],$$

where, k_1 and k_2 are suitably chosen positive constant and V(t) is a continuous function. The derivative of Lyapunov function V(t) concerning time along the solution of the system is,

$$\begin{aligned}\frac{dV(t)}{dt} &= \frac{dN(t)}{dt} + \frac{dA(t)}{dt} + \frac{dP(t)}{dt} + \frac{dI(t)}{dt} = \left\{\frac{-r}{K} + \frac{\omega_2 \ddot{I}}{(a+N(t))(a+\ddot{N})}\right\}(N(t)-\ddot{N})^2 + \omega_1\omega_3 P(t)\\ &\times (N(t)-\ddot{N})(A(t)-\ddot{A}) + \{k_1(e_1\omega_1 - e_3\omega_1\omega_3 A(t)) - \omega_1\}(N(t)-\ddot{N})(P(t)-\ddot{P})\\ &+ \left\{\frac{\omega_2(a-\ddot{N})}{(a+N(t))(a+\ddot{N})} + \frac{k_2 e_2 \omega_2 a}{(a+N(t))(a+\ddot{N})}\right\} \times (N(t)-\ddot{N})(I(t)-\ddot{I}) + \beta(k_2-k_1)(P(t)-\ddot{P})\\ &\times (I(t)-\ddot{I}) + \{k_1 e_3\omega_3(\theta - \omega_1\ddot{N}) - \omega_3(\theta-\omega_1\ddot{N})\}(P(t)-\ddot{P})(A(t)-\ddot{A}).\end{aligned}$$

Taking $k_2 = \frac{\ddot{N}-a}{a e_2}$ and $k_1 = \frac{1}{e_1 - e_3\omega_3 A}$,

$$\begin{aligned}\frac{dV}{dt} \leqslant -\Bigg[&\left\{\frac{r}{K} - \frac{\omega_2\ddot{I}}{(a+N)(a+\ddot{N})} - \frac{\omega_1\omega_3 P}{2}\right\}(N-\ddot{N})^2 + \left\{\frac{(1-k_1e_3)\omega_3(\theta-\omega_1\ddot{N})}{2} - \frac{\omega_1\omega_3 P}{2}\right\}\\ &\times (A-\ddot{A})^2 + \left\{\frac{\beta(k_1-k_2)}{2} + \frac{\omega_2(\theta-\omega_1\ddot{N})(1-k_1e_3)}{2}\right\}(P-\ddot{P})^2 + \frac{\beta(k_1-k_2)}{2}(I-\ddot{I})^2\Bigg].\end{aligned}$$

Now, $\frac{dV}{dt}$ is negative definite if (3.20) holds. □

4. Spatio-temporal model

4.1. Linear stability analysis

We analyze the local stability spatiotemporal model (2.2) using following two-dimensional spatiotemporal perturbation:

$$\begin{aligned}N &= N^* + \sigma_1 \exp(\lambda_k t + i(k_x x + k_y y)) = N^* + \sigma_1 h_1,\ A = A^* + \sigma_2 \exp(\lambda_k t + i(k_x x + k_y y)) = A^* + \sigma_2 h_2,\\ P &= P^* + \sigma_3 \exp(\lambda_k t + i(k_x x + k_y y)) = P^* + \sigma_3 h_3,\ I = I^* + \sigma_4 \exp(\lambda_k t + i(k_x x + k_y y)) = I^* + \sigma_4 h_4,\end{aligned}$$

where, σ_1, σ_2, σ_3 and σ_4 are very small constants, k_x and k_y are the components of the wave number k along x and y direction, respectively, and λ_k is wave length.

Theorem 4.1. *The coexistent state of linearized form of the spatiotemporal model (2.2) is locally asymptotically stable if in addition to Theorem 3.12, the following condition also holds:*

$$c_{11} > \max\left\{\frac{c_{13}c_{31}}{c_{33}}, \frac{-c_{44}c_{22} + c_{14}c_{41}}{2(c_{22}+c_{44})}, \frac{c_{23}c_{32}}{c_{22}}\right\}, \tag{4.1}$$

$$c_{11}D_P + c_{33}D_N < -(D_P + D_N)\min\{c_{44}, c_{22}\}, \tag{4.2}$$

$$-\{\frac{c_{11}c_{22}D_I D_P}{c_{22}c_{44}}\} < D_N D_P < \max\left\{\frac{-(c_{11}+c_{33})D_A D_I}{c_{22}+c_{44}}, \frac{-(c_{11}D_P + c_{33}D_N)D_A D_I}{c_{44}D_A + c_{22}D_I}\right\}, \tag{4.3}$$

$$c_{11}D_A + c_{22}D_N < \min\left\{\frac{c_{14}c_{41}}{c_{44}}, \frac{c_{13}c_{41}D_A}{c_{43}}\right\}, \tag{4.4}$$

$$\frac{c_{31}D_A}{c_{22}D_P} > \max\left\{\frac{c_{41}}{c_{43}}, c_{11} - \frac{c_{23}c_{32}D_N}{c_{22}D_P}\right\}, \tag{4.5}$$

$$c_{11}D_P^2 + c_{22}(D_P^2 + D_N^2) + c_{44}(D_P^2 + D_N^2) + D_N^2 c_{33} < 0. \tag{4.6}$$

Proof. The characteristic equation of the linearized spatiotemporal model (2.2) is,

$$(J - Dk^2 - \lambda_k I)(h_1, h_2, h_3, h_4) = 0, \tag{4.7}$$

where,

$$J = \begin{pmatrix} c_{11} & c_{12} & c_{13} & c_{14} \\ c_{21} & c_{22} & c_{23} & c_{24} \\ c_{31} & c_{32} & c_{33} & c_{34} \\ c_{41} & c_{42} & c_{43} & c_{44} \end{pmatrix}, \quad D = \begin{pmatrix} D_N & 0 & 0 & 0 \\ 0 & D_A & 0 & 0 \\ 0 & 0 & D_P & 0 \\ 0 & 0 & 0 & D_I \end{pmatrix},$$

where, k denotes the wave number, $k^2 = k_x^2 + k_y^2$, and I is the 4×4 identity matrix. The entries of matrix J are given in Theorem 3.12. We write characteristic equation (4.7) in the following form:

$$\det(J - Dk^2 - \lambda_k I) = \lambda_k^4 + \gamma_1(k^2)\lambda_k^3 + \gamma_2(k^2)\lambda_k^2 + \gamma_3(k^2)\lambda + \gamma_4(k^2), \tag{4.8}$$

where,

$$\begin{aligned}
\gamma_1(k^2) &= -\mathrm{Trac}(I - Dk^2) = k^2(D_N + D_A + D_P + D_I) + B_1, \\
\gamma_2(k^2) &= k^4(D_A D_P + D_A D_N + D_P D_N + D_A D_I + D_P D_I + D_N D_I) - k^2(D_N(c_{22} + c_{33} + c_{44}) \\
&\quad + D_A(c_{11} + c_{33})c_{44} + D_P(c_{11} + c_{22} + c_{44}) + D_I(c_{11} + c_{22} + c_{33})) + B_2, \\
\gamma_3(k^2) &= k^6(D_N D_A D_P + D_A D_P D_I + D_N D_A D_I + D_N D_P D_I) - k^4((c_{11} + c_{44})D_A D_P + D_A D_N(c_{33} + c_{44}) \\
&\quad + D_P D_N(c_{22} + c_{44}) + D_A D_I(c_{11} + c_{33}) + D_P D_I(c_{11} + c_{22}) + D_N D_I(c_{33} + c_{22})) \\
&\quad + k^2(D_A(-c_{13}c_{31} + c_{11}c_{33} - c_{14}c_{41} - c_{34}c_{43} + c_{33}c_{44}) + D_P(c_{11}c_{22} - c_{14}c_{41} + c_{11}c_{44} + c_{22}c_{44}) \\
&\quad + D_N(-c_{23}c_{32} + c_{22}c_{33} - c_{34}c_{43} + c_{22}c_{44} + c_{33}c_{44}) \\
&\quad + D_I(c_{11}c_{22} - c_{13}c_{31} - c_{23}c_{32} + c_{11}c_{33} + c_{22}c_{33})) + B_3, \\
\gamma_4(k^2) &= k^8 D_A D_P D_N D_I - k^6(c_{44}D_A D_P D_N + c_{11}D_A D_P D_I + c_{33}D_A D_N D_I) + c_{22}D_P D_N D_I) \\
&\quad + k^4((-c_{14}c_{41} + c_{11}c_{44})D_A D_P + (-c_{34}c_{43} + c_{33}c_{44})D_A D_N + c_{22}c_{44}D_P D_N + (-c_{13}c_{31} \\
&\quad + c_{11}c_{33})D_A D_I + c_{11}c_{22}D_P D_I + (-c_{23}c_{32} + c_{22}c_{33})D_N D_I) + k^2(c_{14}c_{33}c_{41} - c_{13}c_{34}c_{41} \\
&\quad - c_{14}c_{31}c_{43} + c_{11}c_{34}c_{43} + c_{13}c_{31}c_{44} - c_{11}c_{33}c_{44})D_A + (c_{14}c_{22}c_{41} - c_{11}c_{22}c_{44})D_P \\
&\quad + (c_{22}(c_{34}c_{43} - c_{33}c_{44}) + c_{23}c_{32}c_{44})D_N + (c_{13}(c_{22}c_{31} - c_{21}c_{32}) + c_{11}(c_{23}c_{32} - c_{22}c_{33}))D_I + B_4.
\end{aligned}$$

In the given expressions, B_1, B_2, B_3, and B_4 are same as defined in Theorem 3.12,

$$\gamma_1\gamma_2 - \gamma_3 = V_1 k^6 + V_2 k^4 + V_3 k^2 + B_1 B_2 - B_3. \tag{4.9}$$

Here,

$$\begin{aligned}
V_1 &= D_A^2(D_P + D_N + D_I) + D_P^2(D_A + D_N + D_I) + 2D_A D_P D_N + D_N^2(D_A + D_P + D_I) + 2D_A D_P D_I \\
&\quad + 2D_A D_N D_I + 2D_P D_N D_I + D_I^2(D_A + D_P + D_N), \\
V_2 &= -D_A^2(c_{11} + c_{33} + c_{44}) - D_P^2(c_{11} + c_{22} + c_{44}) - D_N^2(c_{22} + c_{33} + c_{44}) - D_I^2(c_{11} + c_{22}c_{33}) \\
&\quad - 2(D_A(D_P + D_N) + D_P(D_N + D_I) + D_I(D_A + D_N))(c_{11} + c_{22} + c_{33} + c_{44}), \\
V_3 &= (2c_{11}c_{22} + c_{22}^2 - c_{13}c_{31} + 2c_{11}c_{33} + 2c_{22}c_{33} + c_{33}^2 - c_{14}c_{41} + 2c_{11}c_{44} + 2c_{22}c_{44} + 2c_{33}c_{44} \\
&\quad + c_{44}^2)D_N + (c_{11}(c_{11} + 2c_{22} + 2c_{33} + 2c_{44}) - c_{23}c_{32} + 2c_{22}c_{33} + c_{33}^2 + 2c_{22}c_{44} + 2c_{33}c_{44} + c_{44}^2)D_A \\
&\quad + (c_{11}(c_{11} + 2c_{22} + 2c_{33} + 2c_{44}) + c_{22}^2 - c_{13}c_{31} - c_{23}c_{32} + 2c_{22}c_{33} - c_{34}c_{43} + 2c_{22}c_{44} + 2c_{33}c_{44} + c_{44}^2)D_P \\
&\quad + (c_{11}(c_{11} + 2c_{22} + 2c_{33} + 2c_{44}) + c_{22}^2 + 2c_{22}c_{33} + c_{33}^2 - c_{14}c_{41} - c_{34}c_{43} + 2c_{22}c_{44} + 2c_{33}c_{44})D_I,
\end{aligned}$$

and $B_1B_2 - B_3$ is given in Theorem 3.12. We see that γ_1 is always positive as dispersion coefficients D_N, D_A, D_P and D_I are always positive and from Theorem 3.12, B_1-B_4 are positive. The first term of γ_3 is always positive, the second term of γ_3, i.e., coefficient of k^4 is positive if it follows (4.2) and (4.3). In the third term γ_3, the first term of k^2 is positive if (4.1) holds. The second term is positive when condition (3) of Theorem 3.12 holds. The third coefficient of k^2 is always positive, the fourth coefficient of k^2 in γ_3 is

positive when (4.1) holds. Further, the first coefficient of γ_4 is always positive, second term, i.e., coefficient of k^6 is positive if condition (4.3) holds, the first coefficient of k^4 in γ_4 is positive when condition (3) of Theorem 3.12 holds. The second and third coefficient of k^4 in γ_4 is positive if (4.1) holds. The last coefficient of k^4 in γ_4 is positive when (4.3) holds. The first, second and third coefficient of k^2 in γ_4 is positive if (4.4)-(4.5) holds. The last coefficient of k^2 in γ_4 is positive if (4.1) holds. The expression of $\gamma_1\gamma_2 - \gamma_3$ is a cubic polynomial in k^2 which is positive if all coefficients of polynomial, i.e., V_1, V_2 and V_3 are positive. It is clear from expression that of V_1 is always positive, from expression of V_2, we see that the coefficient of D_A^2 and D_I^2 and last term in V_2 is positive when condition (1) of Theorem 3.12 holds. The coefficients of D_P^2 and D_N^2 are positive when (4.6) holds. Finally, the coefficient of D_N in V_3 is positive when (4.1) holds and rest of the terms of V_3 are positive if condition (1) of Theorem 3.12 holds. Hence, the expression (4.9) is positive. □

Example 4.2. For the following set of biologically realistic parameter value: $r = 6.1$, $K = 100$, $\omega_1 = 0.01$, $\omega_2 = 0.75$, $\omega_3 = 0.5$, $\theta = 1.42$, $\mu_1 = 0.6$, $\mu_2 = 0.2$, $\mu_3 = 2$, $\beta = 0.2$, $h = 0.1$, $e_1 = 0.9$, $e_2 = 0.6$, $e_3 = 0.2$, $a = 40$, $b = 5$, $D_N = 0.001$, $D_A = 3$, $D_P = 8$, $D_I = 0.003$, $k = 2$, the positive equilibrium $E_7(36.907, 825.297, 8.374, 386.067)$ of 2.2, exists and satisfies the Routh-Hurwitz criterion, i.e, $\gamma_1 = 6304.04458$, $\gamma_2 = 8.125227807602582 \times 10^6 > 0$, $\gamma_3 = 3.0167131116344035 \times 10^7$, $\gamma_4 = 2.181086074368113 \times 10^7$, $\gamma_1\gamma_2 - \gamma_3 = 5.11916 \times 10^{10} > 0$ and $\gamma_1\gamma_2\gamma_3 - \gamma_1^2\gamma_4 + \gamma_3^2 = 1.54344 \times 10^{18} > 0$. Therefore, the system (2.2) is locally asymptotically stable at E_7, if along with the Theorem (3.12), the conditions (4.1)-(4.6) also hold.

4.2. *Turing Instability Analysis*

Theorem 4.3. *The spatiotemporal model system* (2.2) *will perform Turing instability for coexistence state* E_7 *if the following conditions hold:*

(1) $Q_1 < 0$ *or* $(Q_2 < 0$ *and* $Q_2^2 > 3Q_3Q_1)$;

(2) $2Q_2^3 - 9Q_1Q_2Q_3 - 2(Q_2^2 - 3Q_1Q_3)^{\frac{3}{2}} + 27Q_3^2Q_0 < 0$.

Proof. The interior equilibrium for spatiotemporal system (2.2) will become unstable if at least one of eigenvalues of characteristic equation (4.8) is positive. Now, we see that from Theorem (4.1) that γ_1-γ_4 will transform to B_1-B_4 for $k = 0$ and Theorem (3.12) states that the coexistence equilibrium is asymptotic stable in this case. But the equilibrium may become unstable if any of the conditions $\gamma_3(k^2) > 0$, $\gamma_4(k^2)$, $\gamma_1(k^2)\gamma_2(k^2) - \gamma_3(k^2) > 0$ and $\gamma_1(k^2)\gamma_2(k^2)\gamma_3(k^2) - \gamma_1^2(k^2)\gamma_3(k^2) - \gamma_4^2(k^2) > 0$ fails to hold with varying k. Hence, diffusion drives coexistence state towards instability. However, it is clear that γ_1 is always positive. Consequently, instability cannot be occurred by contradicting $\gamma_1(k^2) > 0$. This concludes that diffusion-driven instability may occur due to the failure of any one of the rest of the three conditions. Further, we see from the expression of γ_3 and $\gamma_1(k^2)\gamma_2(k^2) - \gamma_3(k^2)$ that both are cubic function of k^2 and negative when conditions (4.2), (4.4), and (4.6) violate. These expressions can be written in the form $Q(k^2) = Q_3k^6 + Q_2k^4 + Q_1k^2 + Q_0 = 0$, where Q_3 and Q_0 are always positive quantities. The values of coefficients Q_0, Q_1, Q_2, Q_3 for γ_3 and $\gamma_1(k^2)\gamma_2(k^2) - \gamma_3(k^2)$ are same as given in Theorem 4.1. The expression $Q(k^2)$ is negative for some positive real number $k^2 \neq 0$ if $Q(k^2)_{\min}$ is less than zero, where the minimum of $Q(k^2)$ occurs at $k^2 = k_c^2 = \frac{-Q_2 \pm \sqrt{Q_2^2 - 3Q_3Q_1}}{3Q_3}$, which is real and positive if and only if condition (1) of Theorem 4.3 holds. Now $Q(k^2)_{min} = \frac{2Q_2^3 - 9Q_1Q_2Q_3 - 2(Q_2^2 - 3Q_1Q_3)^{\frac{3}{2}} + 27Q_3^2Q_0}{27Q_3^2}$. Which is negative if condition (2) of Theorem 4.3 holds.

For the set of parameter given in Fig. 9, we see that system (2.2) is temporally stable and for the same values in Fig. 1 shows that as wave number k varies, $\gamma_3(k^2)$, $\gamma_4(k^2)$, $\gamma_1(k^2)\gamma_2(k^2) - \gamma_3(k^2)$ does not changes its sign from positive to negative. Further, we have also not found any set of parameters for that these values became negative with the advancement of space. Hence, Turing instability does not occur in the system (2.2). □

4.3. Higher-order stability analysis

This subsection contains the higher-order stability analysis [12] of the system (2.1).

Theorem 4.4. *The constant positive steady state E_7 of the spatial model (2.2) is stable for higher-order spatiotemporal perturbation terms.*

Proof. The model (2.2) can be expressed in the following reaction-diffusion system:

$$\left.\begin{aligned} \frac{\partial N}{\partial t} &= f(N,A,P,I) + D_N\left(\frac{\partial^2 N}{\partial x^2} + \frac{\partial^2 N}{\partial y^2}\right), \frac{\partial A}{\partial t} = g(N,A,P,I) + D_A\left(\frac{\partial^2 A}{\partial x^2} + \frac{\partial^2 A}{\partial y^2}\right), \\ \frac{\partial P}{\partial t} &= l(N,A,P,I) + D_P\left(\frac{\partial^2 P}{\partial x^2} + \frac{\partial^2 P}{\partial y^2}\right), \frac{\partial I}{\partial t} = m(N,A,P,I) + D_N\left(\frac{\partial^2 I}{\partial x^2} + \frac{\partial^2 I}{\partial y^2}\right), \end{aligned}\right\} \tag{4.10}$$

with initial distribution and no-flux boundary condition of the population within the 2D closed domain. The coexistence state of the system (2.1) is spatially homogeneous equilibrium for the system (2.2). We consider that equilibrium E_7 is locally stable for the temporal model and taking following spatial perturbations:

$$N = N^* + s(t,x,y),\ A = A^* + u(t,x,y),\ P = P^* + v(t,x,y),\ I = I^* + w(t,x,y)$$

in system (4.10) near the coexistence state E_7. We expand the temporal part of the system (4.10) in the following form using Taylor's series for only second-order terms:

$$\begin{aligned} \frac{\partial N}{\partial t} &= f_N s + f_A u + f_P v + f_I w + \frac{f_{NN}s^2}{2} + \frac{f_{AA}u^2}{2} + \frac{f_{PP}v^2}{2} + \frac{f_{II}w^2}{2} + f_{NA}su \\ &\quad + f_{NP}sv + f_{NI}sw + f_{AP}uv + f_{AI}uw + f_{PI}vw + D_N\left(\frac{\partial^2 s}{\partial x^2} + \frac{\partial^2 s}{\partial y^2}\right), \end{aligned} \tag{4.11}$$

$$\begin{aligned} \frac{\partial A}{\partial t} &= g_N s + g_A u + g_P v + g_I w + \frac{g_{NN}s^2}{2} + \frac{g_{AA}u^2}{2} + \frac{g_{PP}v^2}{2} + \frac{g_{II}w^2}{2} + g_{NA}su \\ &\quad + g_{NP}sv + g_{NI}sw + g_{AP}uv + g_{AI}uw + g_{PI}vw + D_A\left(\frac{\partial^2 u}{\partial x^2} + \frac{\partial^2 u}{\partial y^2}\right), \end{aligned} \tag{4.12}$$

$$\begin{aligned} \frac{\partial P}{\partial t} &= l_N s + l_A u + l_P v + l_I w + \frac{l_{NN}s^2}{2} + \frac{l_{AA}u^2}{2} + \frac{l_{PP}v^2}{2} + \frac{l_{II}w^2}{2} + l_{NA}su \\ &\quad + l_{NP}sv + l_{NI}sw + l_{AP}uv + l_{AI}uw + l_{PI}vw + D_P\left(\frac{\partial^2 v}{\partial x^2} + \frac{\partial^2 v}{\partial y^2}\right), \end{aligned} \tag{4.13}$$

$$\begin{aligned} \frac{\partial I}{\partial t} &= m_N s + m_A u + m_P v + m_I w + \frac{m_{NN}s^2}{2} + \frac{m_{AA}u^2}{2} + \frac{m_{PP}v^2}{2} + \frac{m_{II}w^2}{2} + m_{NA}su \\ &\quad + m_{NP}sv + m_{NI}sw + m_{AP}uv + m_{AI}uw + f_{PI}vw + D_I\left(\frac{\partial^2 w}{\partial x^2} + \frac{\partial^2 w}{\partial y^2}\right). \end{aligned} \tag{4.14}$$

Further, we will take parabolic spatial perturbations:

$$\begin{aligned} s(t,x,y) &= s(t)\cos(k_x x)\cos(k_y y), & u(t,x,y) &= u(t)\cos(k_x x)\cos(k_y y), \\ v(t,x,y) &= v(t)\cos(k_x x)\cos(k_y y), & w(t,x,y) &= w(t)\cos(k_x x)\cos(k_y y). \end{aligned}$$

Taking these perturbations only for the diffusion part of the system (4.10), we get the following system of four differential equations:

$$\begin{aligned} \frac{\partial s}{\partial t} &= f_N s + f_A u + f_P v + f_I w + \frac{f_{NN}s^2}{2} + \frac{f_{AA}u^2}{2} + \frac{f_{PP}v^2}{2} + \frac{f_{II}w^2}{2} + f_{NA}su \\ &\quad + f_{NP}sv + f_{NI}sw + f_{AP}uv + f_{AI}uw + f_{PI}vw + D_N k^2 s, \end{aligned} \tag{4.15}$$

$$\frac{\partial u}{\partial t} = g_N s + g_A u +_h Pv + g_I w + \frac{g_{NN}s^2}{2} + \frac{g_{AA}u^2}{2} + \frac{g_{PP}v^2}{2} + \frac{g_{II}w^2}{2} + g_{NA}su$$

$$+ g_{NP}sv + g_{NI}sw + h_{AP}uv + h_{AI}uw + h_{PI}vw + D_A k^2 u, \tag{4.16}$$

$$\frac{\partial v}{\partial t} = l_N s + l_A u + l_P v + l_I w + \frac{l_{NN}s^2}{2} + \frac{l_{AA}u^2}{2} + \frac{l_{PP}v^2}{2} + \frac{l_{II}w^2}{2} + l_{NA}su$$
$$+ l_{NP}sv + l_{NI}sw + l_{AP}uv + l_{AI}uw + l_{PI}vw + D_P k^2 v, \tag{4.17}$$

$$\frac{\partial w}{\partial t} = m_N s + m_A u + m_P v + m_I w + \frac{m_{NN}s^2}{2} + \frac{m_{AA}u^2}{2} + \frac{m_{PP}v^2}{2} + \frac{m_{II}w^2}{2} + m_{NA}su$$
$$+ m_{NP}sv + m_{NI}sw + m_{AP}uv + m_{AI}uw + f_{PI}vw + D_I k^2 w. \tag{4.18}$$

Now, we multiply equations (4.15)-(4.18) by $2s$, $2u$, $2v$ and $2w$, respectively and then takes only terms of second order in consideration. Thus, we get the equations for $\frac{\partial s^2}{\partial t}$, $\frac{\partial u^2}{\partial t}$, $\frac{\partial v^2}{\partial t}$, $\frac{\partial w^2}{\partial t}$. Again, we multiply (4.15) by u and (4.16) by s, add them and repeat this process for each pair of equations from (4.15)-(4.18), we get equations for $\frac{\partial us}{\partial t}$, $\frac{\partial vs}{\partial t}$, $\frac{\partial sw}{\partial t}$, $\frac{\partial uv}{\partial t}$, $\frac{\partial uw}{\partial t}$, $\frac{\partial vw}{\partial t}$. Combining equations for $\frac{\partial s}{\partial t}$, $\frac{\partial u}{\partial t}$, $\frac{\partial v}{\partial t}$, $\frac{\partial w}{\partial t}$, $\frac{\partial s^2}{\partial t}$, $\frac{\partial u^2}{\partial t}$, $\frac{\partial v^2}{\partial t}$, $\frac{\partial w^2}{\partial t}$, $\frac{\partial us}{\partial t}$, $\frac{\partial vs}{\partial t}$, $\frac{\partial sw}{\partial t}$, $\frac{\partial uv}{\partial t}$, $\frac{\partial uw}{\partial t}$, $\frac{\partial vw}{\partial t}$ results a system of equation in variables s, u, v, w, s^2, u^2, v^2, w^2, su, sv, sw, uv, uw, and vw. Rewriting this dynamical system in matrix form; $\frac{dY}{dt} = DY$, where, $Y = [s, u, v, w, s^2, u^2, v^2, w^2, su, sv, sw, uv, uw, vw]^T$ and D is 14×14 matrix. The characteristic equation for this system is,

$$|D - \lambda I_{14}| = 0. \tag{4.19}$$

Here, $\lambda = \lambda(k)$ are the eigenvalues of matrix D and I_{14} is 14×14 identity matrix. The stable coexistence state of the system (2.2) reaches instability with the advancement of k if at least one eigenvalue of matrix D is real and positive or pair of complex conjugates eigenvalues with a positive real part. Moreover, at least one eigenvalue with a positive real part implies that spatiotemporal perturbation diverges with the advancement of time. □

5. Numerical simulation

Numerical simulation is essential to support the theoretical analysis. It finds the effect of in-built system parameters on the system's behavior. We will first simulate the temporal system (2.1), and then the spatiotemporal system (2.2). We studied the parameter values of [8, 21, 28–31, 36] and set range for each parameter. The default parameter values for the model are midway through the given range except where the model solution did not occur. We choose the predation rate ω_1, lesser than ω_3 as RHD-infected rabbits are scarce, and alternative prey is readily available for foxes. We take ω_2 more than ω_1 as the total food intake of mange-infected foxes depends only on the rabbits. Further, the conversion coefficients for primary prey are taken more than that of alternative prey, as predation on alternative prey negatively affects fox's health condition. Moreover, the conversion coefficients of infective foxes are lesser than the healthy ones.

Table 1: Range of parameter values for the model (2.1).

parameter	r, b	K	ω_1, ω_2	ω_3	a	μ_1	μ_2
Range	$[0.2, 6.1]$	$[5, 500]$	$[0.01, 4.5]$	$[0.5, 2]$	$[0.2, 40]$	$[0.14, 2.9]$	[0.1,0.98]
parameter	μ_3	e_1, e_2	e_3	β	h	θ	-
Range	$[0.1, 2]$	$[0.1, 0.439]$	$[0.2, 0.8]$	$[0.001, 0.28]$	$[0.1, 2]$	1.42	-

5.1. Temporal model

The numerical simulation of non-diffusive system reveals that for the default parameter set: $r = 6.1$, $K = 100$, $\omega_1 = 0.01$, $\omega_2 = 0.75$, $\omega_3 = 0.5$, $\theta = 1.42$, $\mu_1 = 0.6$, $\mu_2 = 0.2$, $\mu_3 = 2$, $e_1 = 0.9$, $e_2 = 0.6$, $e_3 = 0.2$, $\beta = 0.225$, $h = 0.1$, $a = 40$, $a = 40$, the system 2.1 shows very interesting behaviors as disease transmission coefficient β and hunting rate h varies. For this set, the system 2.1 is asymptotically stable

near the interior equilibrium, as presented in the Fig. 2. If we fix other parameters and vary β from 0.2 to 0.12, the system shows chaotic behavior, as shown in Fig. 3. We have also shown these situations through the Lyapunov spectrum in Fig. 4; we call the largest exponent as Maximal Lyapunov exponent (MLE) predicts the behavior of the dynamical system. A negative (MLE) indicates the system is stable, and a positive one shows that the system is chaotic. If we again reduce β to 0.09, the equilibrium $APFIPE$ appears. Following this for $\beta = 0.001$, the equilibrium $APFWIPE$ appears. We can easily see these conditions in Fig. 8 (b) and 8 (c), respectively. If we increase $\mu_1 = 5.1$ and decrease $\mu_3 = 0.2$, diseased equilibrium appears. We can see this in Fig. 8 (a). We have seen from Fig. 6 that if we vary hunting rate from $h = 0.1$ to $h = 2$, the system (2.1) reaches towards the instability and exhibits Hopf bifurcation near state coexistence state. Again, if we increase the healthy predator natural death rate $\mu_2 = 0.2$ to $\mu_2 = 1.04$ and keep other parameters fixed as in Fig. 8 (b), mange-free equilibrium appears as in Fig. 5.

5.2. *Spatiotemporal model*

This subsection contains the numerical simulation of the diffusive system (2.2). The Fig. 9 shows local stability of the interior equilibrium $E_7(36.907, 825.297, 8.374, 386.067)$ of the system (2.2) for diffusion coefficients $D_N = 0.001$, $D_A = 2$, $D_P = 5$ and $D_I = 0.003$, keeping rest of the parameter values same as in Fig. 2. Here, we choose the diffusion coefficient of rabbit and mange-infected fox very less as they are infective and unable to move far in other spatial locations. The system does not change its stability behavior; if we increase the diffusion coefficient to $D_P = 8$ and then $D_P = 12$, we obtained the same Fig. 9. We see in Fig. 10 that the diffusive system shows chaotic behavior for mange contact rate $\beta = 0.12$. We took the same parameter value as Fig. 9 and found the possibility that one eigenvalue of the characteristic equation (4.19) has a positive real part. For this, we have plotted the largest $Re\lambda(k)$ for the linear system and higher-order system obtained by equations (4.7) and (4.19), respectively, against the wavelength k. We have executed this process to check whether stability behavior varies for a higher-order system, which is shown in Fig. 7.

6. Discussion and conclusion

In this article, we proposed and analyzed the European rabbit-alternative prey-red fox four-compartment dynamical model to find the mange, hunting, and long-term effect of RHD on the rabbit-red fox dynamics worldwide. We obtained conditions for the boundedness of the solution, existence, and stability for the non-diffusive model. We have also analyzed the same eco-epidemiological system with diffusion to understand the effect of diffusion on the system.

The numerical simulation shows that the coexistence equilibrium for the non-diffusive and diffusive model is locally and globally stable under a fixed region of attraction R^4_+ when certain conditions are satisfied. The equilibrium is stable with very few numbers of rabbits and healthy red foxes and many alternative preys and mange-infected foxes, confirming the actual scenario. The main reason is that the abundance of rabbits makes it the fox's primary food. Consequently, the predation is asymptotically high and shifts to alternative prey when rabbits become scarce due to RHD [18, 28]. The high consumption of alternative prey results in adverse changes in the physical condition of foxes, and it started to decline. Also, decreasing rabbit population allows vegetation to recover, subsequently incrementing habitat and shelter for wildlife; hence, predation is considered to have decreased, resulting in an increase in alternative prey species on native fauna [18]. For the critical value of mange contact rate $\beta = \beta_+ = .12$, the system's behavior becomes unpredictable around coexistence equilibrium in both the diffusive and non-diffusive cases. Furthermore, for low disease transmission rate β, only RHD infected rabbit, healthy fox, and mange-infected fox remain in the system. The above results show that mange disease exists in the system environment even at a low disease transmission rate. Moreover, a low mange contact rate helps the healthy red fox population grow, predating the alternative prey population and removing them from the environment. Also, the trivial value of β drives the system to alternative prey-free and mange-free, and only RHD-infected rabbits and healthy foxes are left in the system. We aim to get stable European

rabbit-red fox dynamics despite RHD disease in European rabbits [29]. So, we conclude that we must control mange disease to get the required stable rabbit-red fox dynamics. Mange contact rate can be controlled via isolation and treatment of mange-infected foxes. Also, only diseased populations remain in the environment for a very high alternative prey death rate and low death rate of the mange-infected fox. The system also loses its stability at the critical value of the hunting rate, and bifurcation occurs. The above results that hunting at a significant level destabilizes the dynamics. So, we should control red fox hunting strategies to save the rabbit-alternative prey-fox dynamics. The graphs for the diffusion model show that this system does not have diffusion-driven instability. The reason behind this is the presence of alternative prey in the rabbit-red fox dynamics. Due to RHD's effect, the red fox population finds their primary prey, European rabbits, very few and migrates to other spatial locations searching for alternative prey and easily predates them. So, the system became stable with space. The above concludes that if the proposed system is stable with time, it is also stable with the advancement of space. It is observed from the higher-order stability analysis that the largest $\mathrm{Re}\lambda(k) < 0$ for both the linear system and higher-order for all values of wavelength k, which concludes that if the system is linearly stable, it is also higher-order stable. The advantage of the proposed model is to control the declining red fox population despite RHD in European rabbits by regulating mange contact rate, which is the significant factor of the proposed system. Further, we show that the presence of alternative prey in the dynamic proposed by [29] drives the diffusive system towards stability. This research did not take into account hunting strategies for healthy predators. If we take different hunting rates for healthy and infected predators, we would know which reason more influences the stability, hunting of healthy foxes or mange-infected foxes.

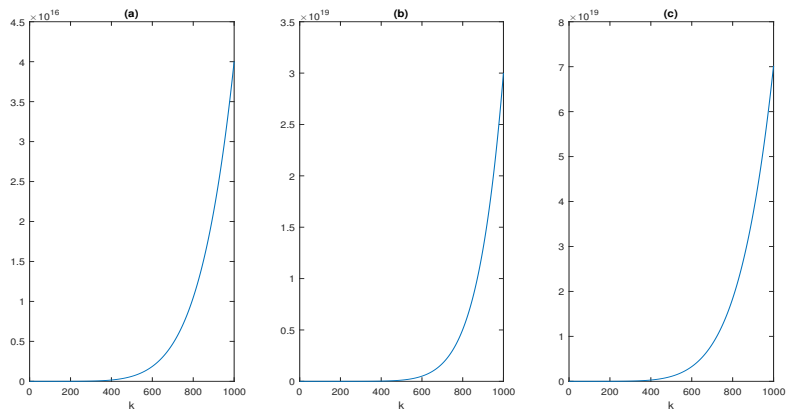

Figure 1: Turing instability for (a) γ_3; (b) γ_4; (c) $\gamma_1\gamma_2 - \gamma_3$.

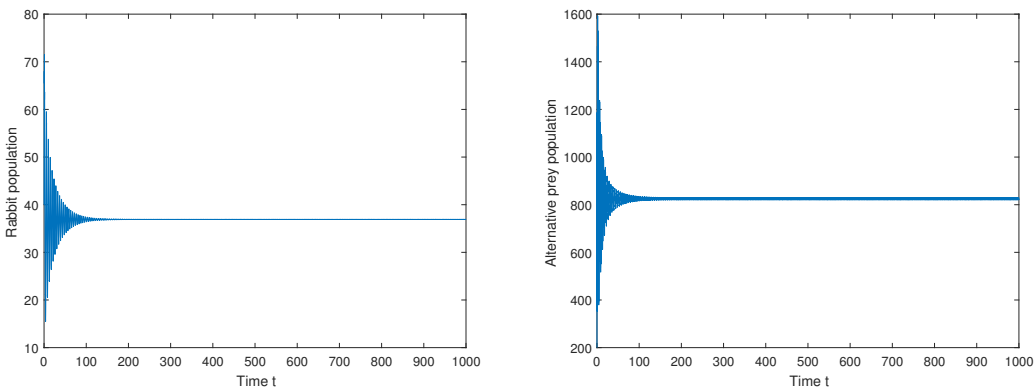

(a) (b)

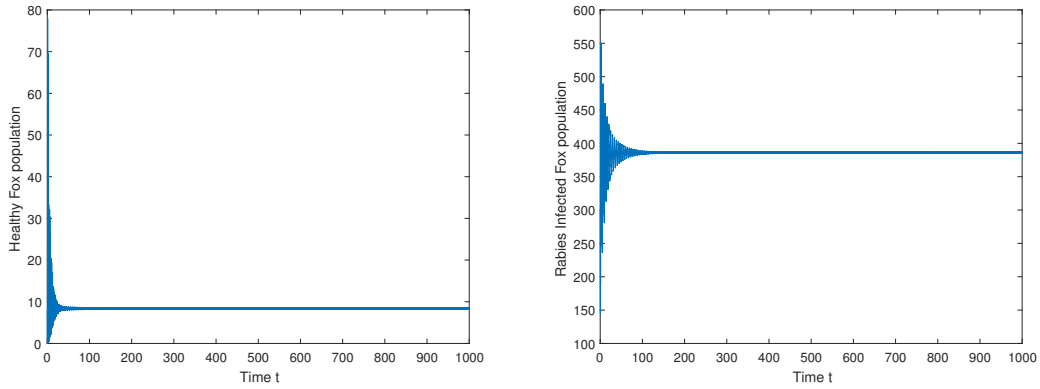

(c) (d)

Figure 2: Stability figure (a) rabbit population; (b) alternative prey population; (c) healthy fox; (d) mange-infected fox; when $r = 6.1$, $K = 100$, $\omega_1 = 0.01$, $\omega_2 = 0.75$, $\omega_3 = 0.5$, $\theta = 1.42$, $\mu_1 = 0.6$, $\mu_2 = 0.2$, $\mu_3 = 2$, $\beta = 0.225$, $h = 0.1$, $e_1 = 0.9$, $e_2 = 0.6$, $e_3 = 0.2$, $a = 40$, $b = 5$, with the initial condition $[N(0)A(0)P(0)I(0)] = [402008300]$.

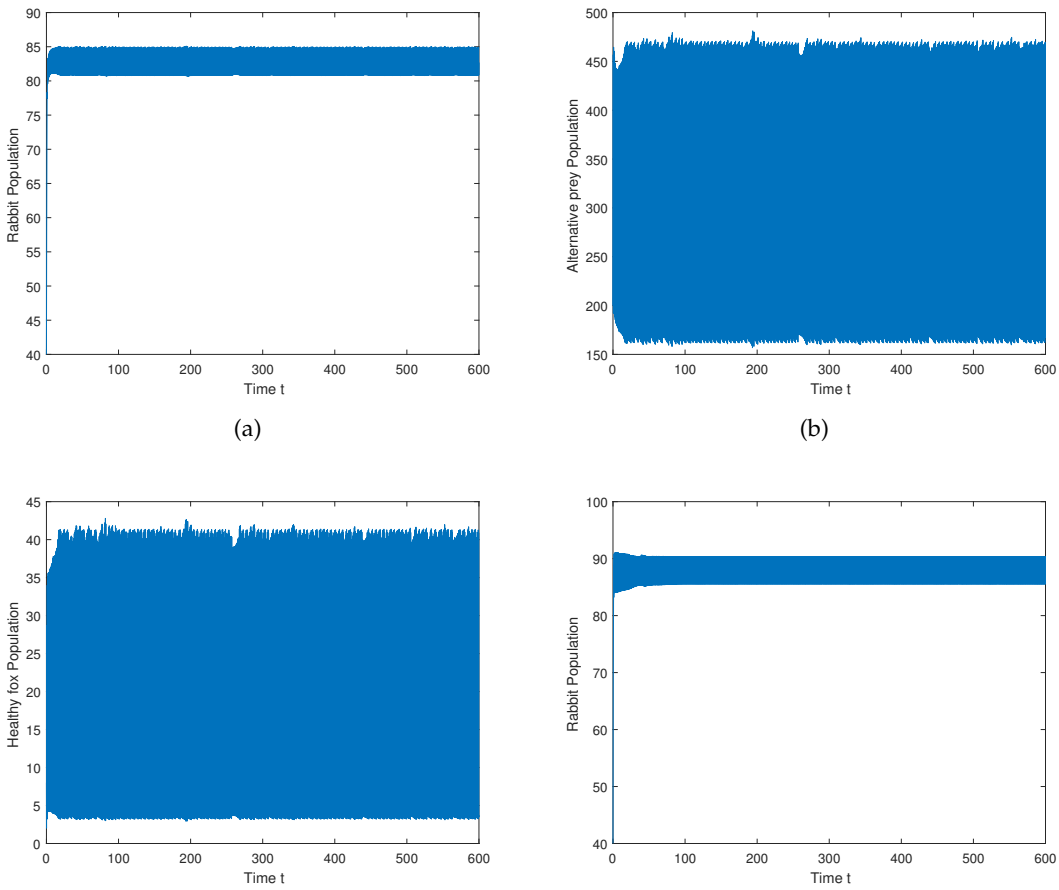

(a) (b)

(c) (d)

Figure 3: Chaotic behavior of (a) rabbit population; (b) alternative prey population; (c) healthy fox; (d) mange-infected fox; for $\beta = 0.12$, keeping rest of the parameters fixed as in Fig. 2.

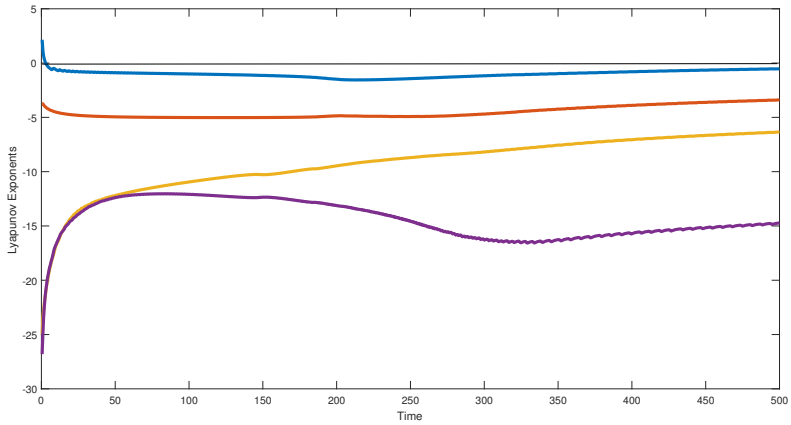

(a)

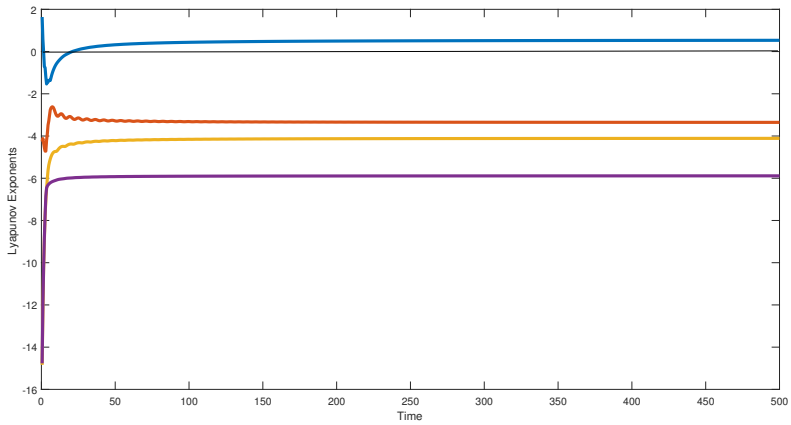

(b)

Figure 4: Convergence plot of Lyapunove spectrum for different values of β and keeping other parameter fixed as 2 (a) stable focus for $\beta = 0.225$ with $(-0.52303, -3.3887, -6.3459, -14.7247)$; (b) strange attractor for $\beta = 0.12$ with $(0.54329, -3.3587, -4.105, -5.886)$.

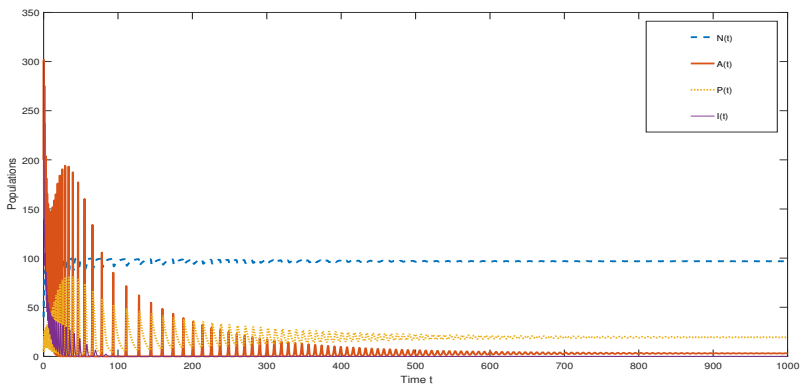

Figure 5: Stability figure of MFE for $\mu_2 = 1.04$ and $\beta = 0.09$, keeping rest of the parameters fixed as in Fig. 2.

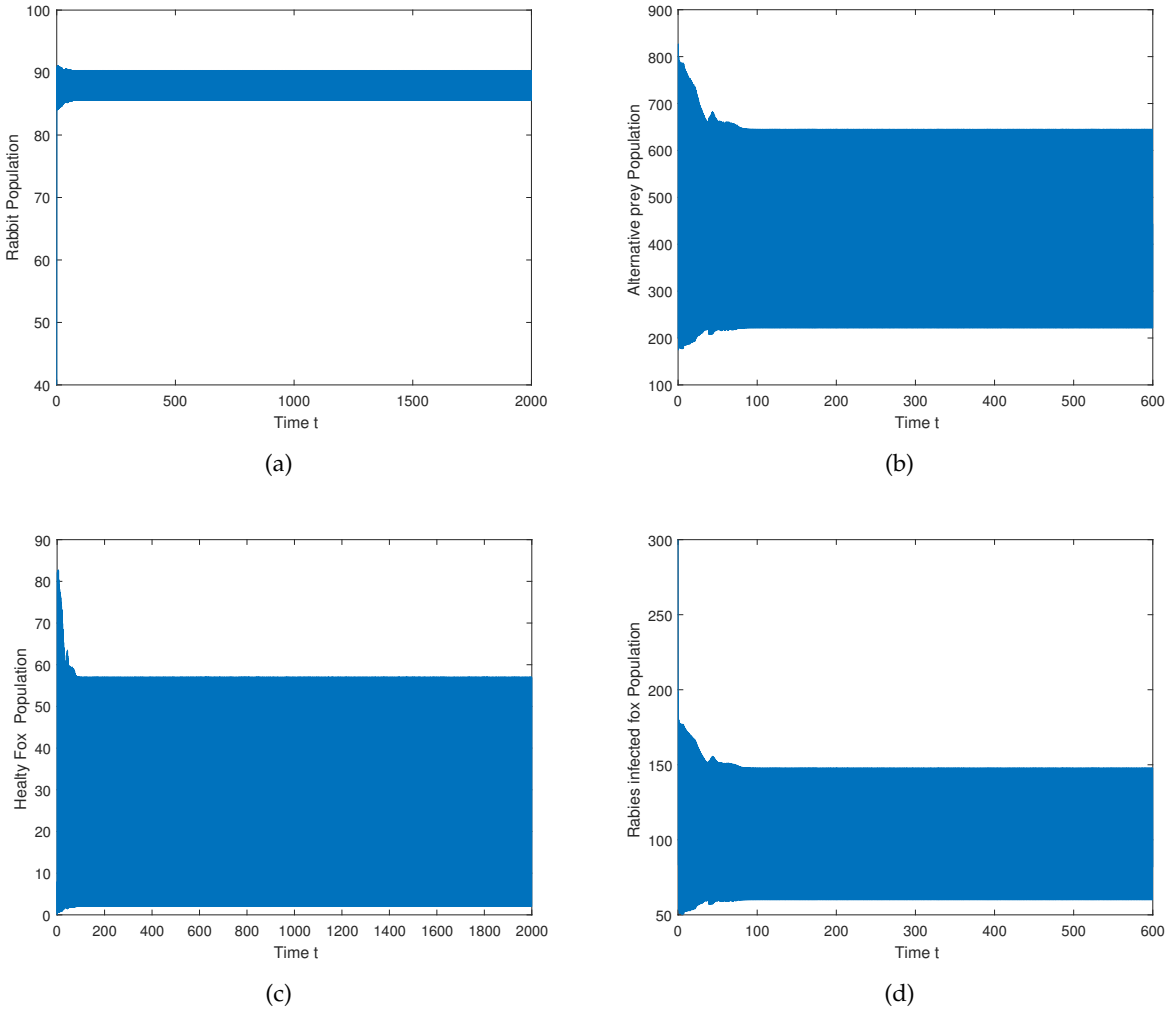

Figure 6: Bifurcation figure (a) rabbit population; (b) alternative prey population; (c) healthy fox; (d) mange-infected fox; for $h = 2$ keeping rest of the parameters fixed as in Fig. 2.

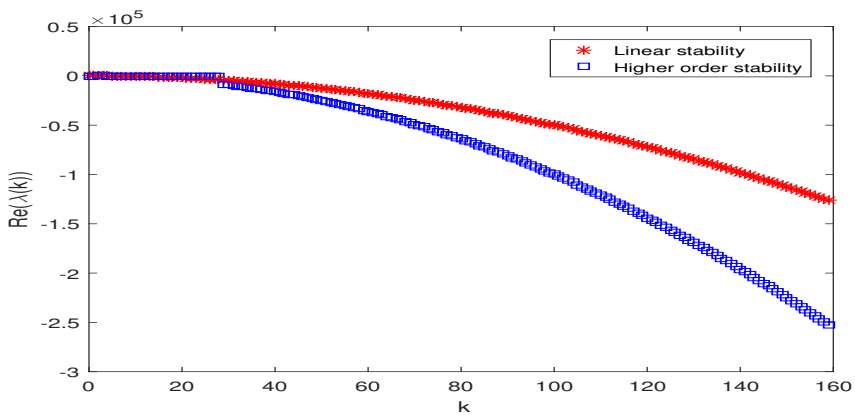

Figure 7: Higher order stability in diffusive model, for $r = 6.1$, $K = 100$, $\omega_1 = 0.01$, $\omega_2 = 0.75$, $\omega_3 = 0.5$, $\theta = 1.42$, $\mu_1 = 0.6$, $\mu_2 = 0.2$, $\mu_3 = 2$, $\beta = 0.225$, $h = 0.1$, $e_1 = 0.9$, $e_2 = 0.6$, $e_3 = 0.2$, $a = 40$, $b = 5$, $D_N = 0.001$, $D_A = 2$, $D_P = 5$, $D_I = 0.003$.

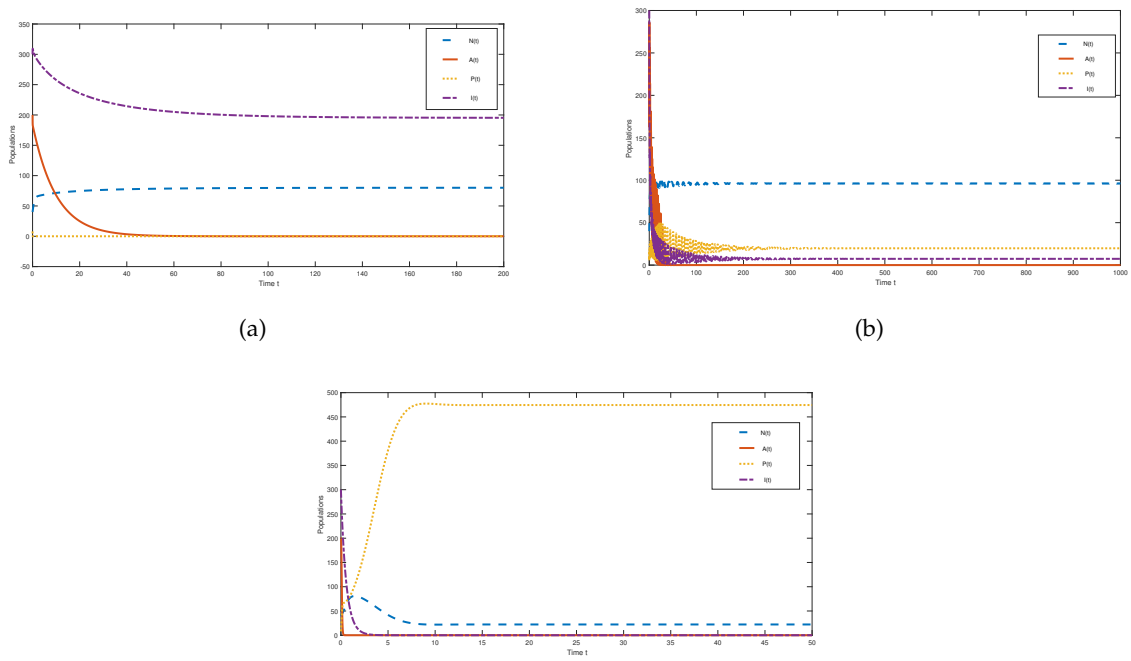

(a) (b)

(c)

Figure 8: Stability figure for (a) diseased equilibrium for $\mu_1 = 5.1$ and $\mu_3 = 0.2$; (b) APFIPE for $\beta = 0.09$; (c) APFWIPE for $\beta = 0.001$, keeping rest of the parameters fixed as in Fig. 2.

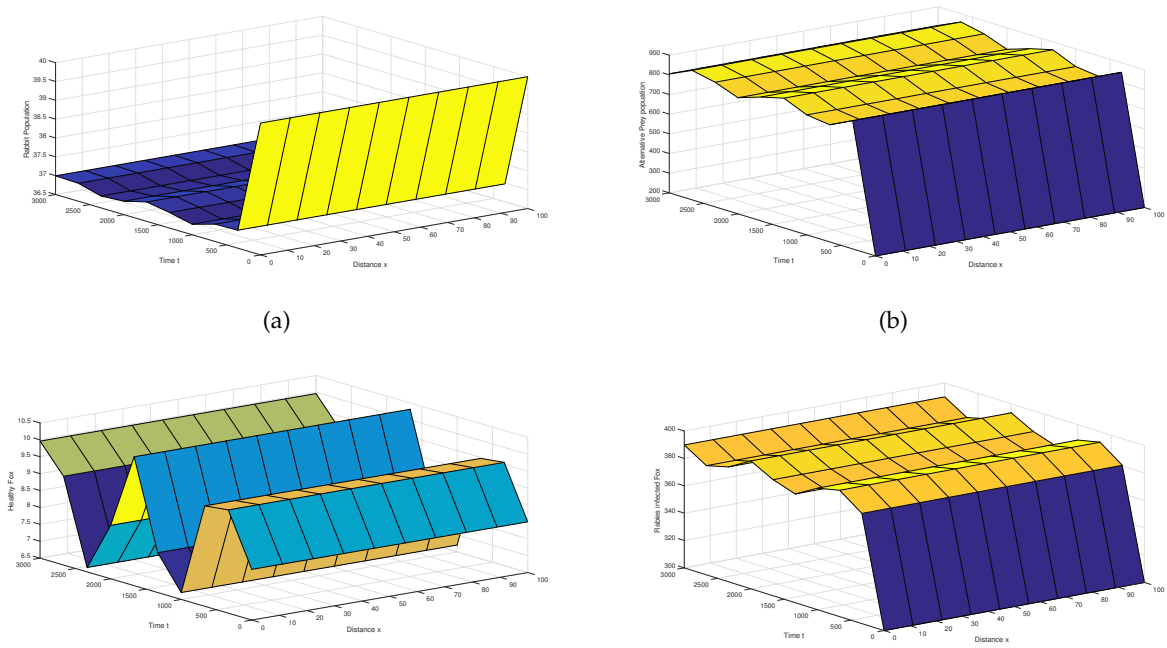

(a) (b)

(c) (d)

Figure 9: Stability figure of diffusive system (a) rabbit population; (b) alternative prey population; (c) healthy fox; (d) mange-infected fox, when $r = 6.1$, $K = 100$, $\omega_1 = 0.01$, $\omega_2 = 0.75$, $\omega_3 = 0.5$, $\theta = 1.42$, $\mu_1 = 0.6$, $\mu_2 = 0.2$, $\mu_3 = 2$, $\beta = 0.2$, $h = 0.1$, $e_1 = 0.9$, $e_2 = 0.6$, $e_3 = 0.2$, $a = 40$, $b = 5$, $D_N = 0.001$, $D_A = 2$, $D_P = 5$, $D_A = 0.003$,with the initial condition $[N(0)A(0)P(0)I(0)] = [402008300]$.

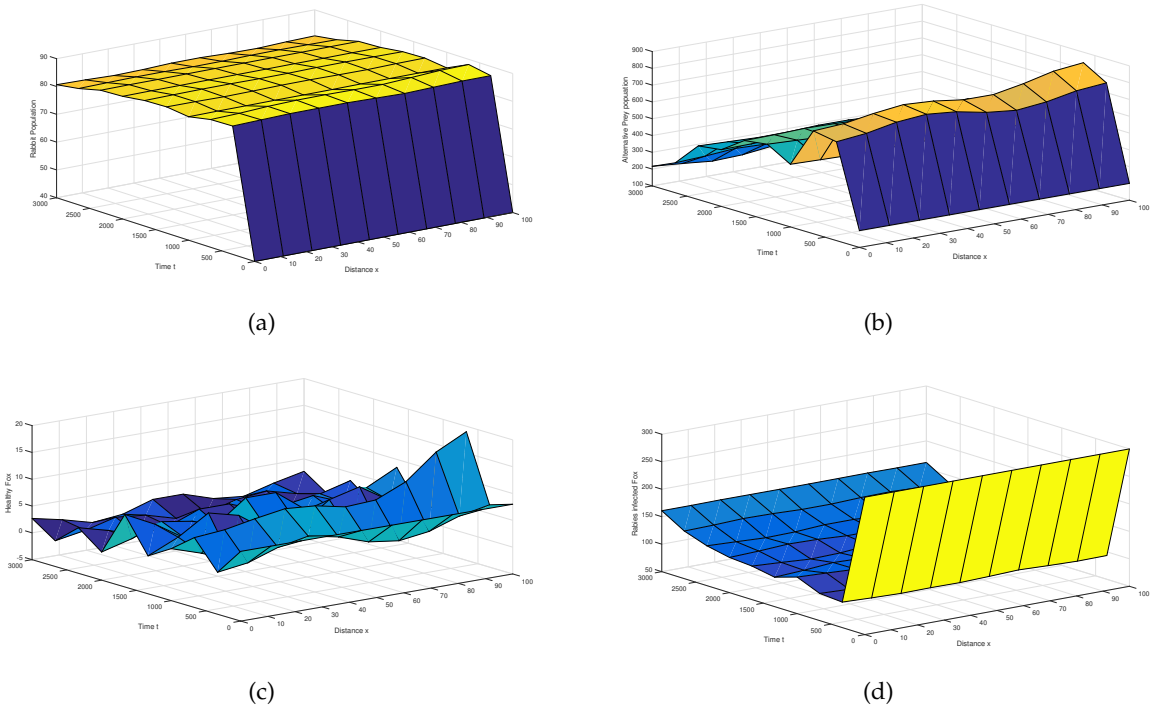

(a) (b)

(c) (d)

Figure 10: Chaotic behavior of diffusive system (a) rabbit population; (b) alternative prey population; (c) healthy fox; (d) mange-infected fox; when $r = 6.1$, $K = 100$, $\omega_1 = 0.01$, $\omega_2 = 0.75$, $\omega_3 = 0.5$, $\theta = 1.42$, $\mu_1 = 0.6$, $\mu_2 = 0.2$, $\mu_3 = 2$, $\beta = 0.12$, $h = 0.1$, $e_1 = 0.9$, $e_2 = 0.6$, $e_3 = 0.2$, $a = 40$, $b = 5$, $D_N = 0.001$, $D_A = 2$, $D_P = 5$, $D_A = 0.003$, with the initial condition $[N(0)A(0)P(0)I(0)] = [401008300]$.

References

[1] E. D. Ables, *Ecology of the red fox in north america*, The wild canids: their systematics, behavioral ecology and evolution, (1975). 1

[2] F. Astorga, S. Carver, E. S. Almberg, G. R. Sousa, K. Wingfield, K. D. Niedringhaus, P. Van Wick, *International meeting on sarcoptic mange in wildlife*, BioMed Central (June 2018, Blacksburg, Virginia, USA), **2018** (2018), 10 pages. 1

[3] P. J. Baker, S. Harris, C. P. Robertson, G. Saunders, P. C. White, *Differences in the capture rate of cage-trapped red foxes vulpes vulpes and an evaluation of rabies control measures in britain*, J. Appl. Ecol., **38** (2001), 823–835. 1

[4] F. Barraquand, L. F. New, S. Redpath, J. Matthiopoulos, *Indirect effects of primary prey population dynamics on alternative prey*, Theor. Popul. Biol., **103** (2015), 44–59. 1

[5] E. Beltrami, T. Carroll, *Modeling the role of viral disease in recurrent phytoplankton blooms*, J. Math. Biol., **32** (1994), 857–863. 1

[6] S. Belvisi, E. Venturino, *An eco epidemic model with diseased predators and prey group defense*, Simul. Model. Pract. Theor., **34** (2013), 144–155. 1

[7] S. P. Bera, A. Maiti, G. P. Samanta, *A prey-predator model with infection in both prey and predator*, Filomat, **29** (2015), 1753–1767. 1

[8] S. Biswas, S. K. Sasmal, S. Samanta, M. Saifuddin, Q. J. A. Khan, J. Chattopadhyay, *A delayed eco-epidemiological system with infected prey and predator subject to the weak allee effect*, Math. Biosci., **263** (2015), 198–208. 1, 5

[9] S. Boutin, *Testing predator prey theory by studying fluctuating populations of small mammals*, Wildlife Research, **22** (1995), 89–99. 1

[10] J. Chattopadhyay, S. Pal, A. E. Abdllaoui, *Classical predator prey system with infection of prey populationa–a mathematical model*, Math. Methods Appl. Sci., **26** (2003), 1211–1222. 1

[11] J. Dawes, M. Souza, *A derivation of hollings type I, II and III functional responses in predator prey systems*, J. Theor. Biol., **327** (2013), 11–22. 2

[12] J. Dhar, R. S. Baghel, *Role of dissolved oxygen on the plankton dynamics in spatiotemporal domain*, Modeling Earth Systems and Environment, **2** (2016), 1–15. 4.3

[13] X. B. Gao, Q. H. Pan, M. F. He, Y. B. Kang, *A predator-prey model with diseases in both prey and predator*, Phys. A, **392** (2013), 5898–5906. 1

[14] K. P. Hadeler, H. I. Freedman, *Predator-prey populations with parasitic infection*, J. Math. Biol., **27** (1989), 609–631. 1

[15] C. Hanlon, J. Childs, *Rabies: Scientific basis of the disease and its management*, Rabies Epidemiology, **2013** (2013), 61–107. 1

[16] M. Haque, E. Venturino, *An ecoepidemiological model with disease in predator: the ratiodependent case*, Math. Methods Appl. Sci., **30** (2007), 1791–1809. 1

[17] H. W. Hethcote, W. Wang, L. Han, Z. Ma, *A predator prey model with infected prey*, Theor. Popul. Biol., **66** (2004), 259–268. 1

[18] C. Holden, G. Mutze, *Impact of rabbit haemorrhagic disease on introduced predators in the flinders ranges*, Wildlife Research, **29** (2002), 615–626. 1, 6

[19] C. S. Holling, *The functional response of predators to prey density and its role in mimicry and population regulation*, The Memoirs of the Entomological Society of Canada, **97** (1965), 5–60. 2

[20] Y. H. Hsieh, C.-K. Hsiao, *Predator-prey model with disease infection in both populations*, Math. Med. Biol.: J. IMA, **25** (2008), 247–266. 1

[21] Z. Y. Hu, Z. D. Teng, C. J. Jia, L. Zhang, X. Chen, *Complex dynamical behaviors in a discrete eco-epidemiological model with disease in prey*, Adv. Difference Equ., **2014** (2014), 19 pages. 5

[22] E. J. Kormondy, *Concepts of ecology*, Prentice-Hall, New York, (1969). 3.2

[23] M. Kot, *Elements of mathematical ecology*, Cambridge University Press, Cambridge, (2001). 2

[24] M. Y. Li, L. C. Wang,*A criterion for stability of matrices*, J. Math. Anal. Appl., **225** (1998), 249–264. 3.3

[25] E. Lyznarova, S. Pekar, *Metabolic specialisation on preferred prey and constraints in the utilisation of alternative prey in an ant-eating spider*, Zoology, **119** (2016), 464–470. 1

[26] J. D. Murray, *Mathematical biology*, Springer-Verlag, Berlin, (1989). 2

[27] K. pada Das, K. Kundu, J. Chattopadhyay, *A predator prey–mathematical model with both the populations affected by diseases*, Ecolog. Complex., **8** (2011), 68–80. 1

[28] R. P. Pech, G. M. Hood, *Foxes, rabbits, alternative prey and rabbit calicivirus disease: consequences of a new biological control agent for an outbreaking species in australia*, J. Appl. Ecol., **35** (1998), 434–453. 1, 5, 6

[29] P. Roy, R. K. Upadhyay, *Assessment of rabbit hemorrhagic disease in controlling the population of red fox: A measure to preserve endangered species in australia*, Ecolog. Complex., **26** (2016), 6–20. 1, 3.8, 3.9, 3.3, 6

[30] S. Sharma, G. P. Samanta, *A leslie-gower predator-prey model with disease in prey incorporating a prey refuge*, Chaos Solitons Fractals, **70** (2015), 69–84. 1, 3.3

[31] H. Singh, J. Dhar, H. S. Bhatti, *Dynamics of a prey-generalized predator system with disease in prey and gestation delay for predator*, Modeling Earth Systems and Environment, **2** (2016), 9 pages. 1, 5

[32] J. Sooknanan, B. Bhatt, D. Comissiong, *A modified predator–prey model for the interaction of police and gangs*, Royal Soc. Open Sci., **3** (2016), 16 pages. 2

[33] C. D. Soulsbury, G. Iossa, P. J. Baker, N. C. Cole, S. M. Funk, S. Harris, *The impact of sarcoptic mange sarcoptes scabiei on the british fox vulpes vulpes population*, Mammal Review, **37** (2007), 278–296. 1

[34] C. Tannoia, E. Torre, E. Venturino, *An incubating diseased-predator ecoepidemic model*, Journal of Biological Physics, **38** (2012), 705–720. 1

[35] R. K. Upadhyay, S. R. K. Iyengar, *Introduction to mathematical modeling and chaotic dynamics*, CRC Press, Boca Raton, (2013). 3.2

[36] R. K. Upadhyay, P. Roy, C. Venkataraman, A. Madzvamuse, *Wave of chaos in a spatial eco-epidemiological system: Generating realistic patterns of patchiness in rabbit lynx dynamics*, Math. Biosci., **281** (2016), 98–119. 5

[37] E. Venturino, *The influence of diseases on lotka-volterra systems*, Rocky Mountain J. Math., **24** (1994), 381–402. 1

[38] E. Venturino, *The effects of diseases on competing species*, Math. Biosci., **174** (2001), 111–131. 1

[39] R. Villafuerte, C. Calvete, J. Blanco, J. Lucientes, *Incidence of viral hemorrhagic diseasein wild rabbit populations in spain*, Mammalia, **59** (1995), 651–660. 1

[40] M. Zaccaroni, N. Biliotti, M. Caroli, E. Sereni, F. Dessy-Fulgheri, *Effect of fox hunting with small hound packs on spatial behaviour of brown hares*, Acta Theriolog., **57** (2012), 257–260. 1